

AD-A189 842

HIGH SPEED BANDPASS SAMPLING OF DIGITAL COMMUNICATIONS
WAVEFORMS(U) AIR FORCE INST OF TECH WRIGHT-PATTERSON
AFB OH SCHOOL OF ENGINEERING T E KEITH DEC 87

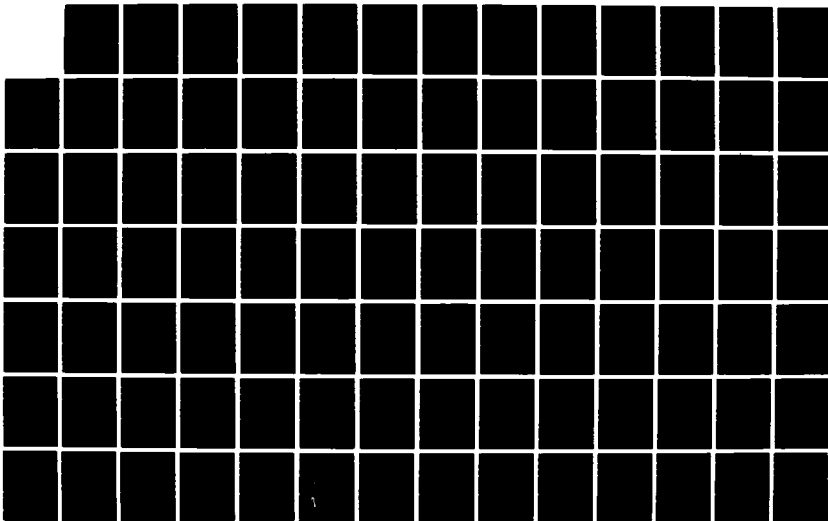
1/2

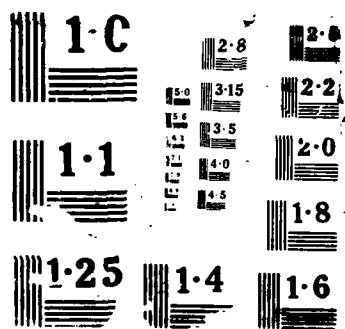
UNCLASSIFIED

AFIT/DE/ENG/87D-31

F/G 14/2

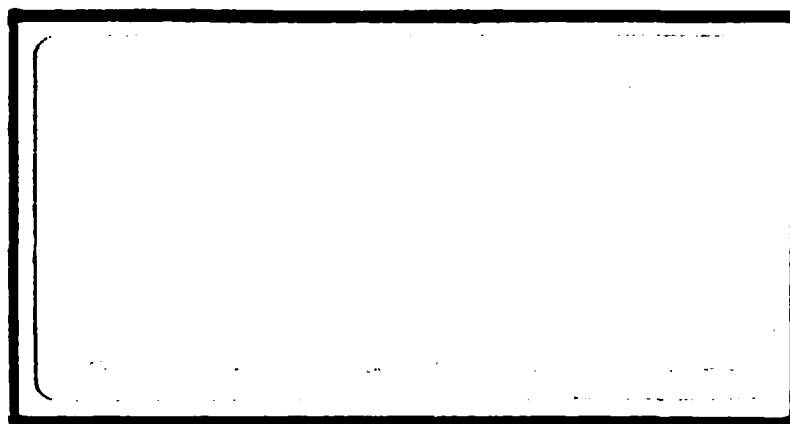
ML





DTIC FILE COPY

AD-A189 842



DTIC
ELECTE
MAR 07 1988
S H

DEPARTMENT OF THE AIR FORCE
AIR UNIVERSITY
AIR FORCE INSTITUTE OF TECHNOLOGY

Wright-Patterson Air Force Base, Ohio

DISTRIBUTION STATEMENT A

Approved for public release

88 3 01 109

1

HIGH SPEED, BANDPASS SAMPLING OF
DIGITAL COMMUNICATIONS WAVEFORMS

THESIS

Tommy E. Keith
Captain, USAF

AFIT/GE/ENG/87D-31

DTIC
ELECTE
MAR 07 1988
H

DISTRIBUTION STATEMENT A

Approved for public release
distribution is unlimited

AFIT/GE/ENG/87D-31

HIGH SPEED, BANDPASS SAMPLING OF
DIGITAL COMMUNICATIONS WAVEFORMS

THESIS

Presented to the Faculty of the School of Engineering
of the Air Force Institute of Technology

Air University

In Partial Fulfillment of the
Requirements for the Degree of
Master of Science in Electrical Engineering

Tommy E. Keith, B.S.E.E.

Captain, USAF

December 1987

Approved for public release; distribution unlimited

Acknowledgments

In accomplishing the task outlined in this thesis I had help from a great many people. I am indebted to my thesis advisor Dr. (Major) Glenn Prescott for suggesting the subject of this document and for taking the time to answer all my many questions. I would also like to thank my readers, Major Dale Hibner and Captain Rob Williams, and my sponsors, Ms. Dianne Summers and Lieutenant Rick Oddo. I especially want to thank my wife Becky for all the love and support she has given me while working on this document.



Accession For	
NTIS	✓
DTIC	✓
Uncl.	✓
Dist.	✓
By	
Date	
Auth.	
Dist.	
A-1	

Table of Contents

	Page
Acknowledgments	ii
List of Figures	v
List of Tables	vii
Abstract	viii
I. Introduction	1
Problem	1
Scope	1
Background	1
Approach	7
II. Theoretical Analysis	8
Introduction	8
Shannon's Low-Pass Sampling Theorem .	9
Proof 1	10
Proof 2	12
Aliasing	17
Direct Sampling	21
Introduction	21
Conventional Direct Sampling	21
Analysis	23
First-Order Sampling	30
Analysis	31
Pth-Order Sampling	37
Introduction	37
Pth-Order Sampling Analysis	38
Second-Order Sampling Analysis	40
Conventional Quadrature Sampling	44
Introduction	44
Analysis	44
Summary	47
Quadrature Sampling	47
Introduction	47
Case i	48
Case ii	51
Case iii	53
Summary	57
Complex Sampling	58
Introduction	58
Analysis	58
Summary	61
Chapter Summary	61

III. Results	62
Introduction	62
Conventional Quadrature Sampling	65
Quadrature Sampling	67
Complex Sampling	85
IV. Conclusions and Recommendations	86
Conclusions	86
Recommendations	86
Bibliography	88
Vita	90

List of Figures

Figure	Page
1. Digital Processing Receiver	1
2. Typical Bandpass Waveform	2
3. Direct Sampling	3
4. Second-Order Sampling	4
5. Conventional Quadrature Sampling	4
6. Quadrature Sampling	5
7. Complex Sampling	6
8. Typical Low-Pass Signal	9
9. Low-Pass Sampling Operation	14
10. Ideal Low-Pass Filter	15
11. Example of Aliasing	16
12. Low-Pass Sampling Process	18
13. Speech Signal With Interference	19
14. Example of Noise Folding Down	20
15. Bandpass Sampling Process	22
16. Direct Sampling - f_s for Three Different Cases	24
17. Determining $f_{s(\min)}$	26
18. $w_{s(\min)}$ as a Function of w_o and σ	27
19. Bandpass Transfer Pair	29
20. Embedding Technique For First-Order Sampling ...	36
21. Second-Order Sampling	42
22. Sample Trains For Second-Order Sampling	43
23. Conventional Quadrature Sampling	46
24. Quadrature Sampling	48

25. Embedding Technique - Case ii	53
26. Embedding Technique - Case iii	56
27. Complex Sampling	59
28. Fourier Transform of an Analytic Signal	61
29. Bandpass Signal for $2f_0 = kW$ ($k = \text{integer}$)	70
30. Bandpass Signal for $2f_0 \neq kW$ ($k = \text{integer}$)	73
31. Q vs K with $L = 1$ - Persons' Example	76
32. Q vs K with $L = 1$ - Small Timing Errors	78
33. Q vs K with $L = 1$ - Large Timing Errors	79
34. Q vs K with $L = 1.5$	82
35. Q vs K with $L = 2.0$	83
36. Q vs K with $L = 5.0$	84

List of Tables

Table	Page
I. Comparison of Timing Errors	81

Abstract

The purpose of this thesis is to investigate and analyze bandpass sampling techniques. Bandpass sampling theory is shown to be an extension of the Shannon low-pass sampling theory. Five bandpass sampling techniques are investigated: direct sampling (also called first-order sampling), p th-order sampling (in particular second-order sampling where $p=2$), conventional quadrature sampling, quadrature sampling, and complex sampling (also called Hilbert transform sampling).

Direct sampling is a single channel approach to bandpass sampling while the other approaches require two channels. The two channel techniques offer a sampling rate reduction of up to one half over direct sampling, but there are trade-offs to consider when choosing a two channel technique. It is shown that the effects of random phase error can render the conventional quadrature sampling approach useless. Timing is critical with quadrature sampling. Reconstruction error, due to hardware timing errors, is shown to be directly proportional to the center frequency and is a function of the bandwidth of the signal. Plots were developed to show the effect of timing on a given bandpass signal when the center frequency and the bandwidth are known.

I. INTRODUCTION

Problem

The purpose of this thesis is to investigate and analyze various bandpass sampling techniques.

Scope

This thesis considers direct sampling (also called first-order sampling), 2nd-order sampling, quadrature sampling, and complex sampling (sampling using Hilbert Transforms). There are various implementations of each technique and at times these categories overlap. The details will be presented in Chapter II.

Background

In a digital processing receiver the received signal is sampled, quantized, and processed by a digital processor. The signal may be sampled at any point in the RF or IF portions of the receiver. A block diagram of a digital processing receiver is shown in Figure 1.

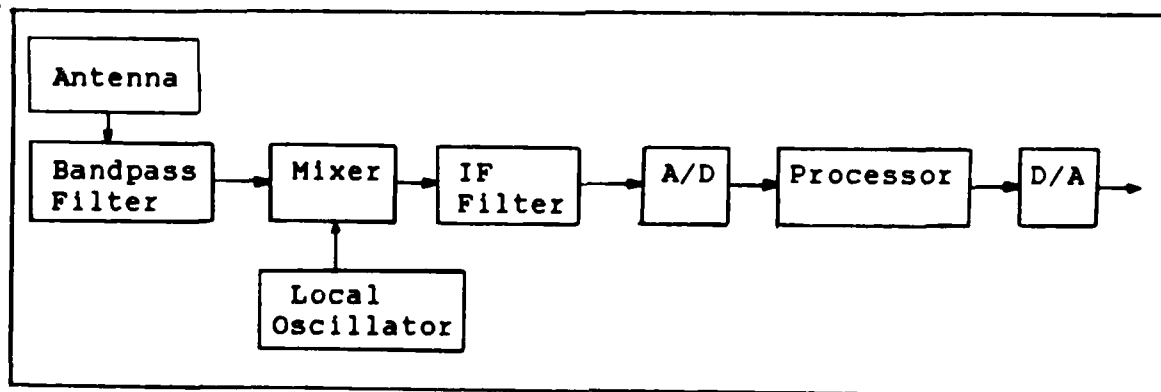


Figure 1. Digital Processing Receiver

For this thesis, uniform sampling is assumed to occur in the IF stage. The resulting sampled spectrum may either be a real bandpass spectrum or a complex low-pass spectrum depending upon the sampling technique employed.

If a band-limited waveform is sampled at a uniform and sufficiently high rate, the original waveform can be reconstructed from the sampled values by appropriate interpolating functions. Shannon showed that the minimum sampling rate is equal to twice the highest frequency component of the waveform (9:519). However, for bandpass waveforms like the one shown in Figure 2, it is theoretically possible to sample at a rate of σ/π samples/s, or twice the bandwidth of the bandpass waveform. Thus, depending upon the bandpass sampling technique used, the sampling rate for a bandpass signal can be much lower than twice the highest frequency.

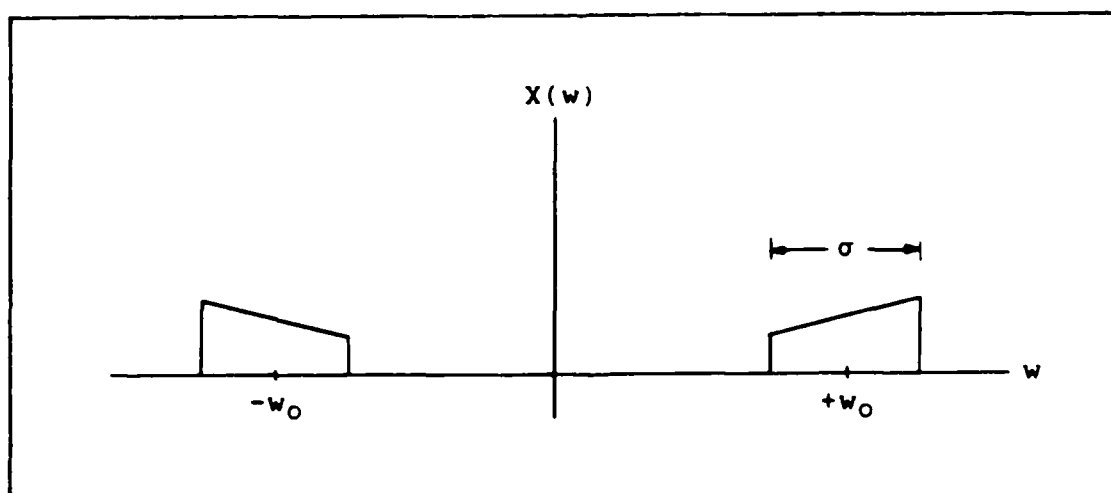


Figure 2. Typical Bandpass Waveform (13:907)

Direct sampling, as shown in Figure 3, involves multiplying the bandpass waveform with a train of uniformly spaced pulses. The spacing of the pulses (or the sampling rate) is governed by the bandwidth of the bandpass waveform. Special consideration needs to be given to the sampling rate to avoid the problem of aliasing. It will be shown that for direct sampling of the bandpass waveform the minimum sampling rate, f_s samples/s, ranges from twice the bandwidth to four times the bandwidth and is a function of the relationship between the center frequency and the bandwidth. This will be examined further in Chapter II.

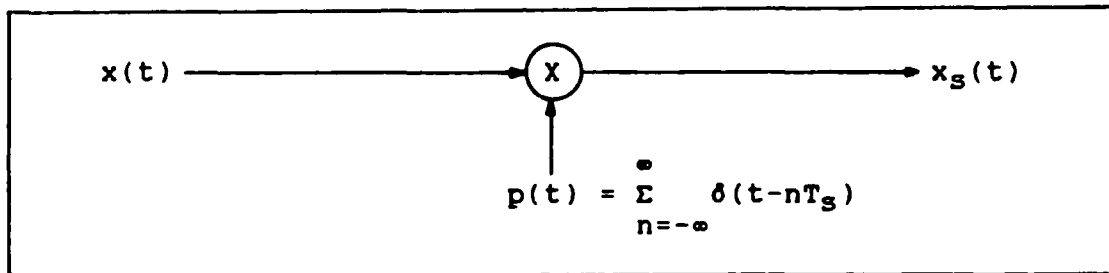


Figure 3. Direct Sampling (10:16)

p th-order sampling is an extension of direct sampling. Where direct sampling involves a single train of uniformly separated samples of the bandpass waveform, p th-order sampling involves p trains of samples as shown in Figure 4 for the special case of $p=2$. The trains are slightly displaced in time but occur at the same frequency (10:40). The sampling rate for each of the p channels is f_s/p samples/s for an average rate of f_s samples/s.

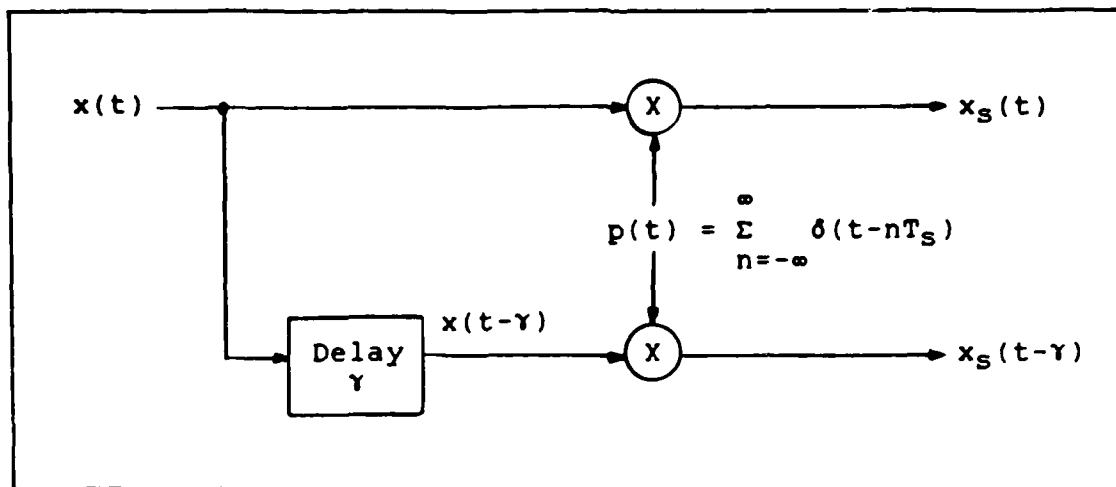


Figure 4. Second-Order Sampling (13:905)

Two implementations of quadrature sampling will be discussed. The first, from this point on to be referred to as conventional quadrature sampling, is sketched in Figure 5.

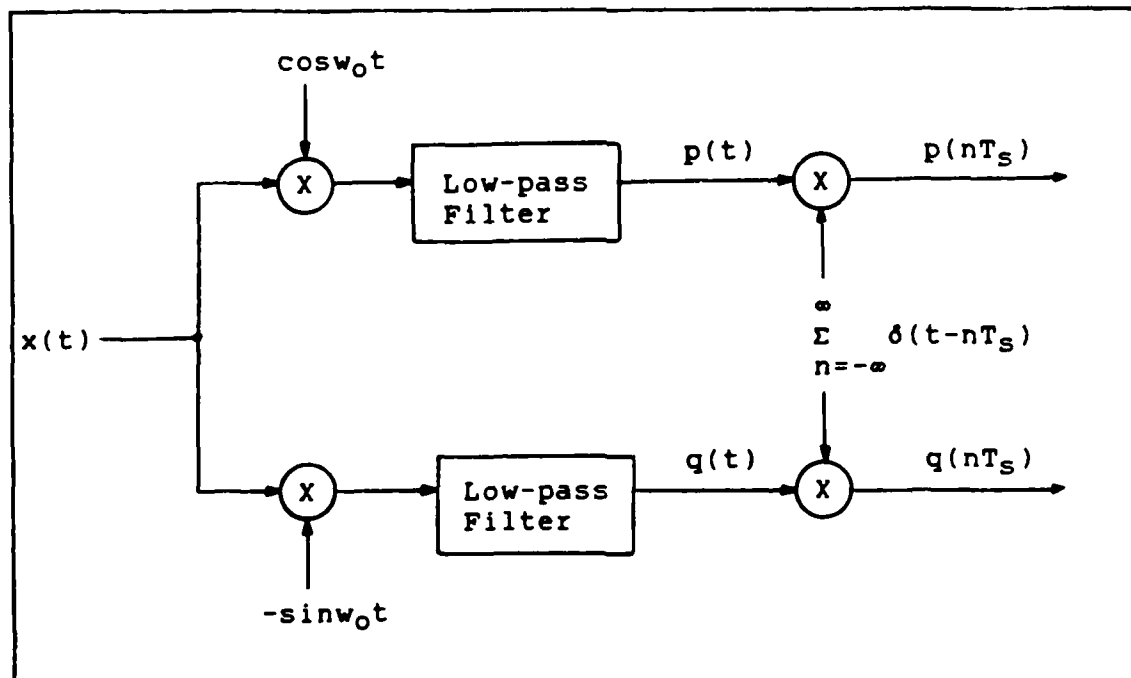


Figure 5. Conventional Quadrature Sampling (10:37)

Here, the bandpass signal is preprocessed by employing quadrature demodulation prior to sampling. In one channel $x(t)$ is modulated by $\cos \omega_0 t$ and low-pass filtered to remove the sum frequency term to obtain the in-phase component, $p(t)$. Similarly, the quadrature component, $q(t)$, is obtained from the sine channel. Because of the preprocessing of $x(t)$, the components $p(t)$ and $q(t)$ can be sampled according to the low-pass sampling theorem. The original waveform, $x(t)$, can be reconstructed from samples of the low-pass components.

The second implementation of quadrature sampling, from here on referred to as simply quadrature sampling, was introduced by O.D. Grace and S.P. Pitt, and is an application of second-order sampling (pth-order sampling where $p=2$). Quadrature sampling, pictured in Figure 6, requires uniform sampling of both the bandpass signal and its quarter wavelength (based on nominal frequency ω_0) translation, each at a common sampling rate depending upon the exact relationship between ω_0 and σ (the bandwidth).

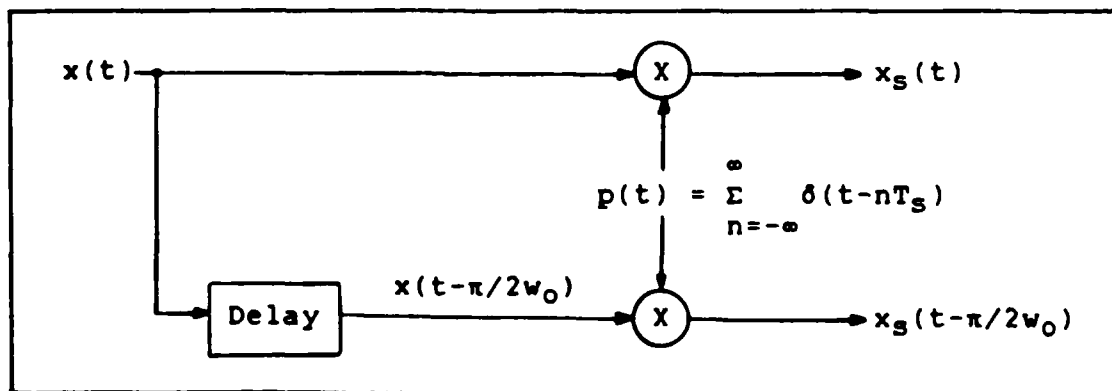


Figure 6. Quadrature Sampling

When the intersample spacing is properly chosen, the bandpass signal can be reconstructed in its entirety from knowledge of the sample values; moreover, with quadrature sampling, the (low-pass) in-phase and quadrature components of the bandpass signal have a simple explicit representation in terms of samples of the original bandpass signal without the preprocessing required in conventional quadrature sampling. It will be shown that the minimum sampling rate for quadrature sampling can be as low as σ/π (average) samples/s (2:1659,1662).

Another possibility for maintaining the (average) sampling rate equal to its minimum value σ/π samples/s is to sample both the bandpass waveform, $x(t)$, and its Hilbert transform, $x_H(t)$, at a rate of $\sigma/2\pi$ samples/s. This approach, pictured in Figure 7, is called complex sampling (10:37-38).

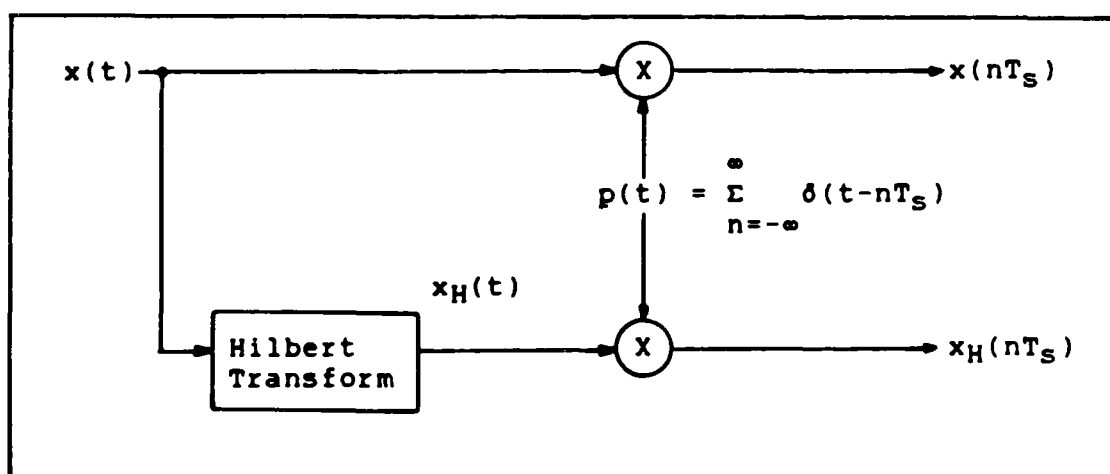


Figure 7. Complex Sampling (13:905).

Approach

The approach to this thesis was basic: analyze the bandpass sampling techniques from a theoretical standpoint and draw conclusions from the analysis.

In chapter II, a theoretical analysis of each bandpass sampling technique will be presented.

Results of the analysis will be presented in Chapter III.

Finally, in chapter IV, conclusions are drawn based upon the theoretical analysis presented in Chapter II and the results detailed in Chapter III.

II. THEORETICAL ANALYSIS

Introduction

The conversion of signals from analog to digital representation involves two operations: sampling and quantization. With regard to sampling, one of the principle requirements is that it be sufficiently fast to represent the waveform adequately (4:91). But how do you determine what is "sufficiently fast?" For low-pass signals the question is easily answered with the Shannon sampling theorem (15:43). For bandpass signals, sampling is a little more complicated. A direct application of the Shannon theorem will work, but there are several techniques available that allow us to sample bandpass signals at rates much lower than twice the highest frequency component in the signal. The purpose of this thesis is to investigate and analyze bandpass sampling theory and to examine the various techniques that can be used to implement bandpass sampling. This chapter is devoted to the development of the bandpass sampling techniques from a theoretical standpoint.

The best approach to the topic of bandpass sampling is to begin with a review of the Shannon sampling theorem. As mentioned, this theorem primarily concerns low-pass signals, but its results easily extend to the bandpass case. In addition, by reviewing low-pass sampling theory, sampling

issues such as aliasing and fold-down (to be discussed later in this chapter - and again in Chapter III) can be addressed early, before examining the individual bandpass sampling techniques. It will be shown that the aliasing and fold-down issues are basically handled the same whether talking about low-pass sampling or bandpass sampling.

The approach in this chapter will be to consider the low-pass sampling theorem first. That result will be extended to the bandpass case. Then the individual bandpass sampling techniques, mentioned briefly in chapter one, will be discussed.

Shannon's Low-Pass Sampling Theorem. Shannon's theorem states that a signal whose Fourier Transform is zero outside the interval $|w| > B$ as in Figure 8, can be uniquely represented by a set of samples of the waveform taken at intervals of π/B seconds; i.e., the original waveform can be completely reconstructed from its samples. The sampling frequency, $f_s = B/\pi$, is twice the highest frequency present in the waveform and is usually referred to as the Nyquist frequency (4:91).

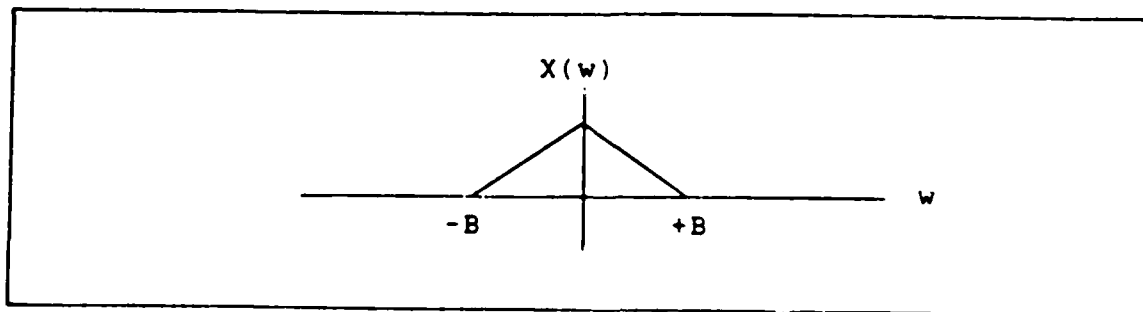


Figure 8. Typical Low-Pass Signal (4:92)

Since this sampling theorem is so significant to the understanding of bandpass sampling theory, two different proofs will be presented here (15:43,46). However, the proofs are not mathematically rigorous, and for our purpose, only the key concepts as they apply to bandpass sampling will be reviewed here.

Proof 1. Assume $X(w)$ is only non-zero along the finite interval $-B < w \leq B$, and expand it in a Fourier Series as

$$X(w) = \sum_{n=-\infty}^{\infty} c_n \exp\{jnt_0 w\} \quad (1)$$

where,

$$t_0 = 2\pi/2B \quad (2)$$

$$c_n = (1/2B) \int_{-B}^B X(w) \exp\{-jnt_0 w\} dw \quad (3)$$

Also, the Fourier inversion formula tells us that

$$x(t) = (1/2\pi) \int_{-B}^B X(w) \exp\{j\omega t\} d\omega \quad (4)$$

Comparing Eq (3) with Eq (4) we find that

$$c_n = (\pi/B)x(-nt_0) = (\pi/B)x[-n\pi/B] \quad (5)$$

This says that the c_n are known once $x(t)$ is known at the points $t = n\pi/B$. Plugging these values of c_n into the series expansion for $X(w)$, Eq (1), we find that

$$X(\omega) = (\pi/B) \sum_{n=-\infty}^{\infty} x(-n\pi/B) \exp\{j\omega n\pi/B\} \quad (6)$$

Eq (6) is essentially a mathematical statement of the sampling theorem. It states that $X(\omega)$ is completely known and determined by the sample values, $x(-n\pi/B)$. These are the values of $x(t)$ at equally spaced points in time. We can plug this $X(\omega)$, given by Eq (6), into the inverse Fourier integral, Eq (4), to find $x(t)$ in terms of its samples. This will yield the following result:

$$x(t) = (1/2\pi) \sum_{n=-\infty}^{\infty} (\pi/B) \int_{-B}^B x(-n\pi/B) \exp\{j\omega n\pi/B\} \exp\{j\omega t\} d\omega \quad (7)$$

or, after simplifying

$$x(t) = \sum_{n=-\infty}^{\infty} x(-n\pi/B) [\sin(Bt+n\pi)/(Bt+n\pi)] \quad (8)$$

The original signal, $x(t)$, may be exactly reconstructed by interpolating samples spaced $t = n\pi/B$ apart. In other words, if we have a signal $x(t)$ with no spectral energy beyond limit B , all information about the signal is contained in a sequence of samples taken at a uniform rate greater than B/π samples/s. Note Eq (8) has the form

$$x(t) = \sum_{k=-\infty}^{\infty} x(kT_s) h(t-kT_s) \quad (9)$$

where T_s is the period between samples taken periodically at times kT_s , $x(kT_s)$ are the samples, and $h(t)$ is the low-pass filter, or the sampling (interpolation) function

$$h(t) = (\sin Bt)/Bt \quad (10)$$

Notice that $h(t)$ has the form $\sin x/x$, whose transform is a spectral window centered about zero. (The importance of this spectral window will be more obvious after Proof 2.) Eq (9) will be referenced throughout this chapter.

Although this proof was straightforward and it gives us $x(t)$ in terms of its samples, it provides little insight into the sampling process. A more intuitive approach is considered in Proof 2, which follows.

Proof 2. Assume once again that $x(t)$ has the transform $X(w)$ which is band limited to the interval $-B < w < B$ as in Figure 8. Next consider the product of $x(t)$ with a periodic train of delta functions, $p(t)$, where

$$p(t) = \sum_{n=-\infty}^{\infty} \delta(t-nT_s) \quad (11)$$

The sifting property of the impulse function tells us that

$$\sum_{n=-\infty}^{\infty} x(t)\delta(t-nT_s) = \sum_{n=-\infty}^{\infty} x(nT_s)\delta(t-nT_s) \quad (12)$$

Using this property, we find that the sampled version of $x(t)$, $x_s(t)$, is given by

$$x_s(t) = x(t)p(t) \quad (13)$$

$$x_s(t) = \sum_{n=-\infty}^{\infty} x(t)\delta(t-nT_s) \quad (14)$$

$$x_s(t) = \sum_{n=-\infty}^{\infty} x(nT_s)\delta(t-nT_s) \quad (15)$$

Figure 9 illustrates the relationship of $x(t)$ and $x_s(t)$; i.e., $x_s(t)$ is $x(t)$ sampled at intervals of T_s .

To show that $x(t)$ can be recovered from $x_s(t)$, we can use the frequency convolution theorem to get

$$x_s(t) = x(t)p(t) \longleftrightarrow (1/2\pi)X(w)*P(w) = X_s(w) \quad (16)$$

where

* denotes convolution

$$P(w) = (2\pi/T_s) \sum_{n=-\infty}^{\infty} \delta(w-nw_s) \quad (17)$$

and

$$w_s = 2\pi/T_s \quad (18)$$

Recall that convolution with a delta function simply shifts the original function. Therefore,

$$\sum_{n=-\infty}^{\infty} X(w)*\delta(w-nw_s) = \sum_{n=-\infty}^{\infty} X(w-nw_s) \quad (19)$$

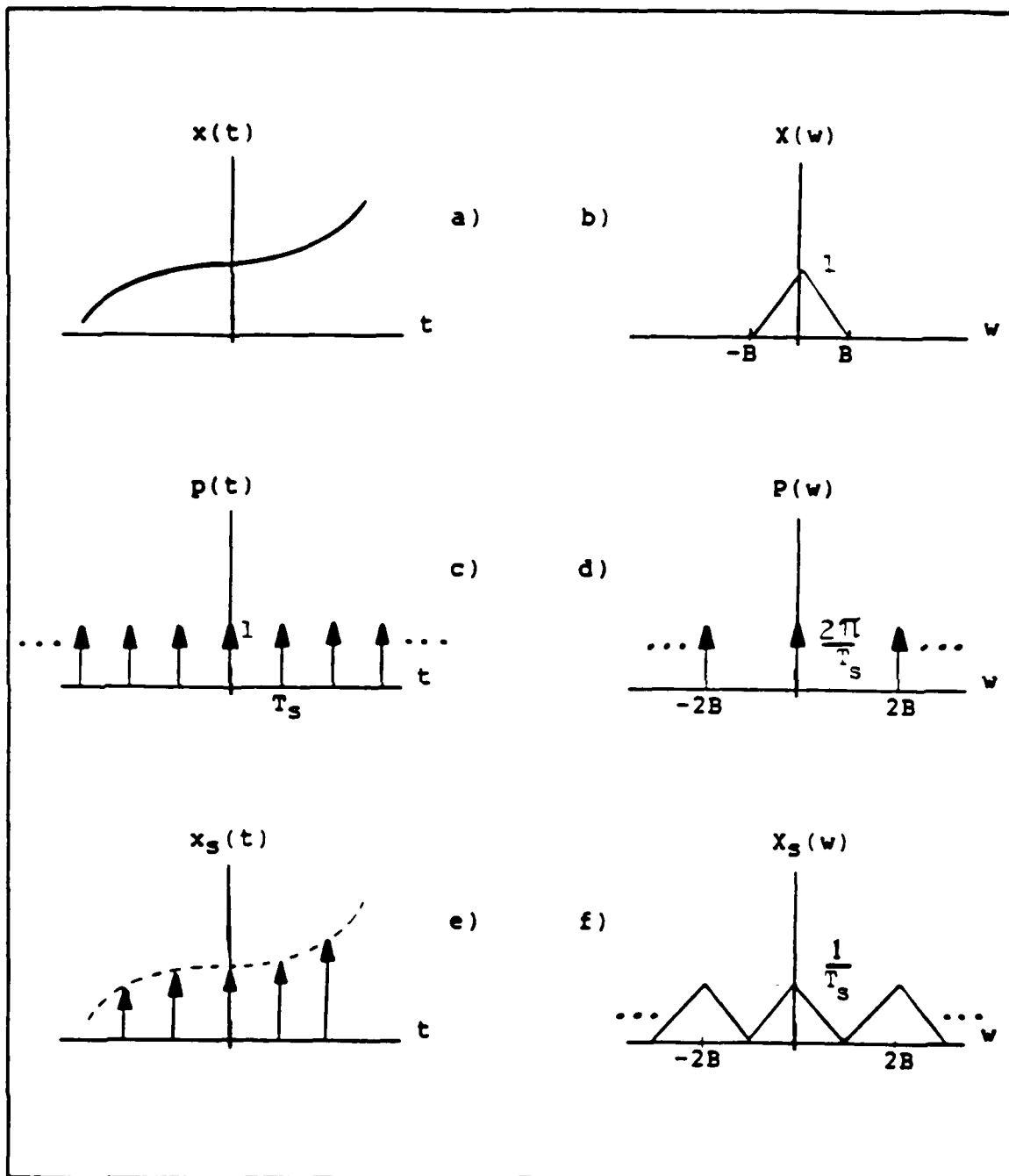


Figure 9. Low-Pass Sampling Operation (15:46)

$$X_S(w) = (1/2\pi)X(w) * (2\pi/T_S) \sum_{n=-\infty}^{\infty} \delta(w-nw_S) \quad (20)$$

$$X_S(w) = (1/T_S) \sum_{n=-\infty}^{\infty} X(w-nw_S) \quad (21)$$

This $X_S(w)$ is sketched in Figure 9. From the sketch of $X_S(w)$ it is clear that $X(w)$ can be identified. In practice, we need only filter $X_S(w)$ with the ideal low-pass filter, $H(w)$, shown in Figure 10, to recover $X(w)$. This is the spectral window referred to in Proof 1. The window function passes all frequency components in the interval $-B \leq w \leq B$ and rejects all others.

In Figure 9f the assumption was made that the "humps" in the figure do not overlap. The sampling rate is set at twice the bandwidth, or $f_s = B/\pi$ samples/s. Figure 11 is a sketch of $X_S(w)$ with $f_s > \sigma/\pi$ samples/s and $f_s < \sigma/\pi$ samples/s. To prevent overlapping spectra the point labeled " $w_s - B$ " must fall to the right of that labeled " B ." If this were not true as in Figure 11c, the result would be undersampling, or aliasing. When aliasing occurs,

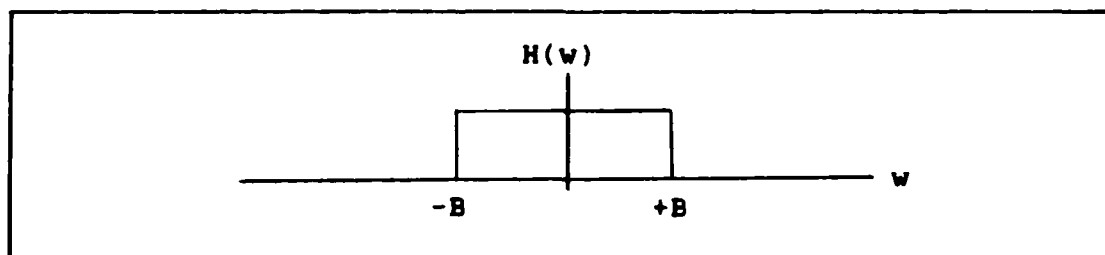


Figure 10. Ideal Low-Pass Filter (9:518)

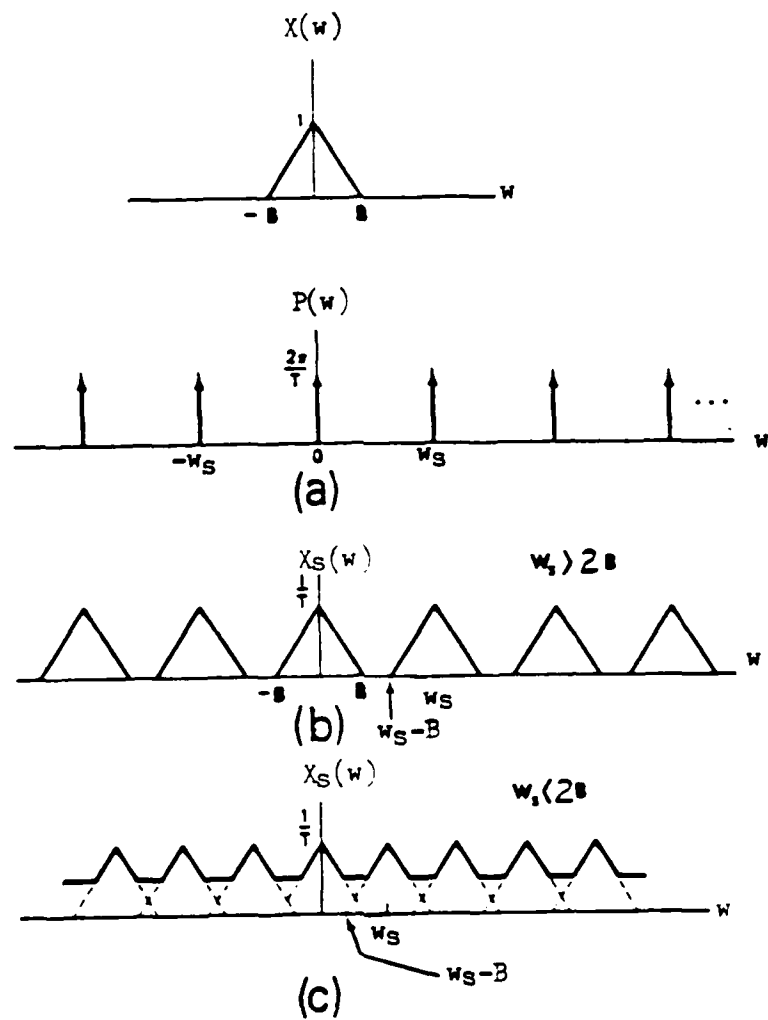


Figure 11. Example of Aliasing (9:517)

it is impossible to uniquely recover $X(\omega)$ by ideal filtering or any other means. This restriction can be rewritten as follows

$$\omega_s - B > B \quad \text{<----->} \quad \omega_s > 2B \quad (22)$$

Since

$$\omega_s = 2\pi/T_s \quad (23)$$

this restriction becomes

$$T_s < \pi/B \quad (24)$$

In other words the samples cannot be spaced any further apart than π/B samples.

Simply stated, the Shannon sampling theorem requires that $x(t)$ be sampled at a rate greater than twice the highest frequency component in $x(t)$ in order to be able to recover the original signal from the sampled data form. This process is summarized in Figure 12.

Aliasing. Aliasing plays an important role in bandpass sampling just as in low-pass sampling. To be able to recover the original signal from the sampled data, none of the shifted spectral components can overlap. This makes bandpass sampling theory a bit more complicated because now two spectral bands are involved in the bandpass case (one at $+\omega_0$ and one at $-\omega_0$ as in Figure 2) as opposed to only one in the low-pass case (from $-B$ to $+B$ as in Figure 8).

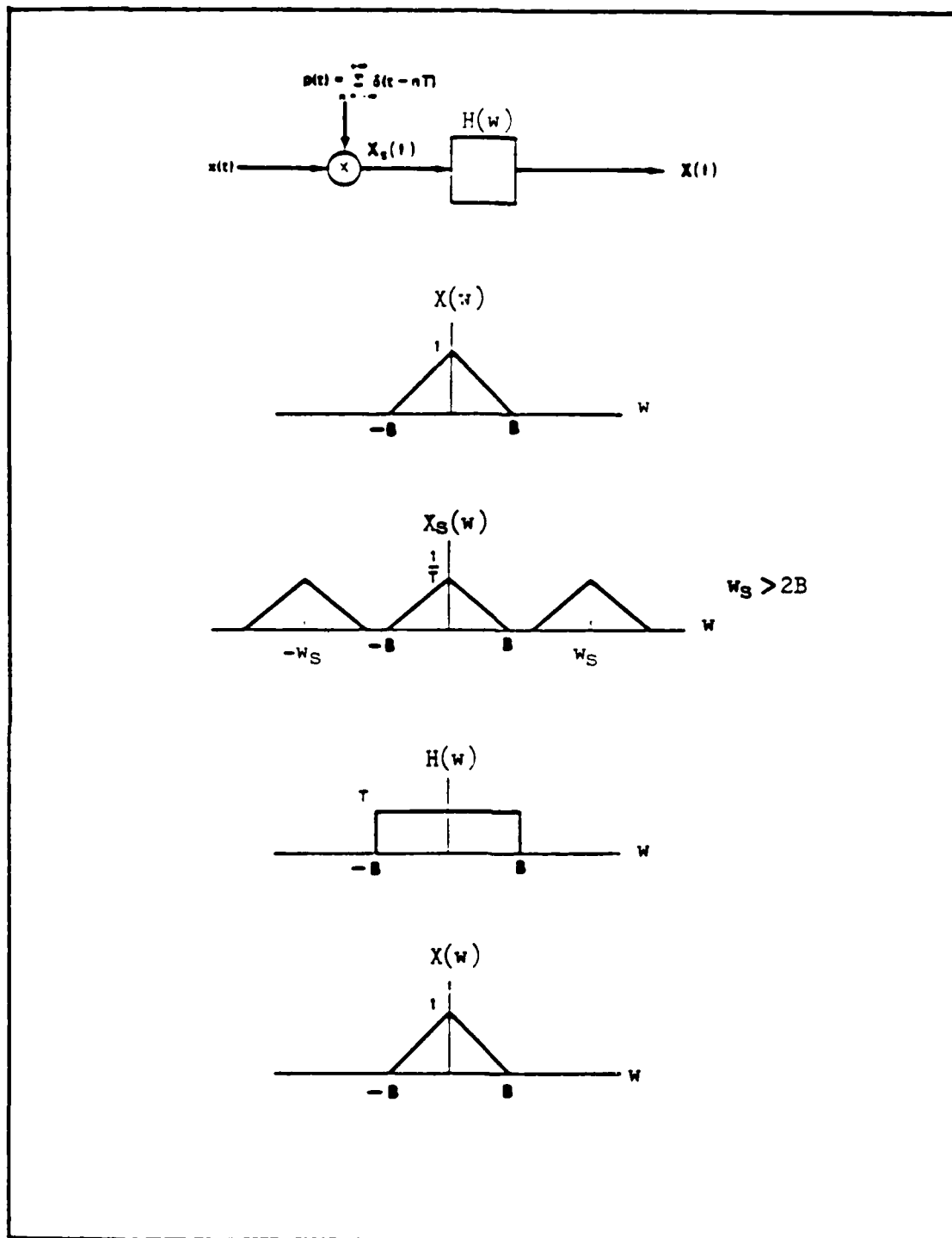


Figure 12. Low-Pass Sampling Process (9:518)

Aliasing can occur if either the signal is not bandlimited or if the sampling rate is too low. Theoretically, if a signal is not bandlimited, there is no way to avoid the aliasing problem with the basic scheme just discussed. However, the spectra of most realizable signals may be assumed to be bandlimited. Furthermore, a common practice is to filter the continuous time signal before sampling to ensure that it does meet the band-limited criterion. These anti-aliasing filters are also important in preventing the possibility of noise or interference folding into the spectrum occupied by our signal (16:47).

The use of antialiasing filters is best illustrated with an example. Assume the speech signal in Figure 13 is confined to the frequency interval between 0.3 and 3.0kHz. Additionally, there is interference at 6kHz. Our concern is what happens to the 6kHz sine wave as a result of sampling? If the composite signal is sampled at 8kHz (a standard in telecommunications), the 6kHz noise will be folded to (or replicated about) the 2kHz position as in Figure 14. The

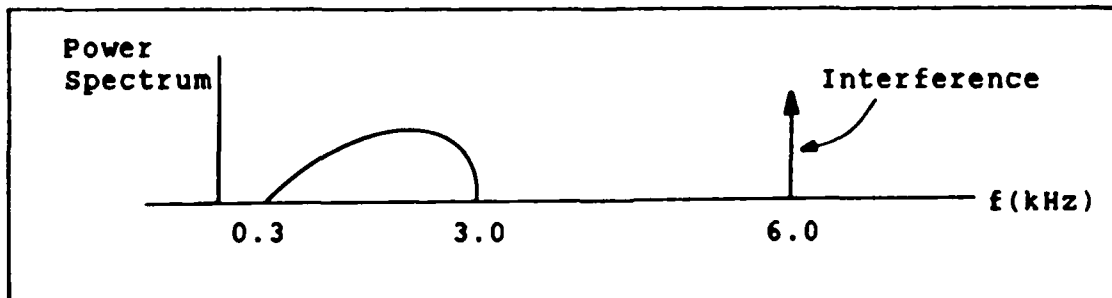


Figure 13. Speech Signal With Interference (12:63)

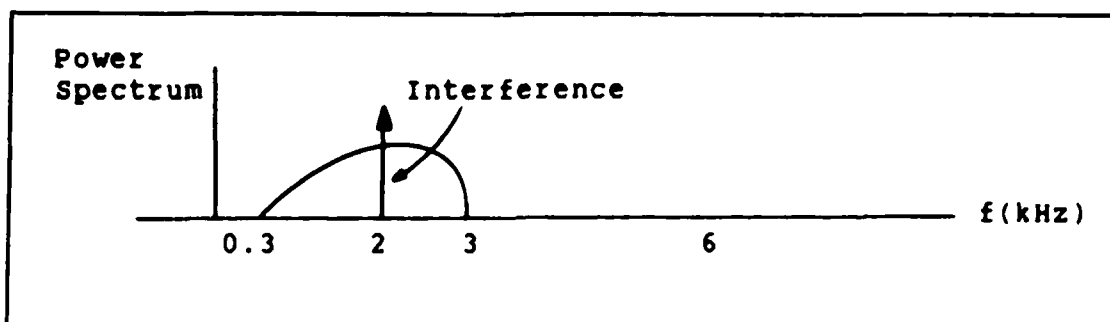


Figure 14. Example of Noise Folding Down (12:64)

interfering signal cannot be removed without loss of a portion of the original speech signal. The noise could, however, be removed prior to sampling by filtering the speech signal (12:63-64). This antialiasing process serves two important functions: it artificially bandlimits the signal being sampled; and, it filters out noise which could otherwise fold down and make signal recovery impossible (14:52). More will be said about antialiasing in Chapter III.

This background material lays the necessary foundation for discussing the individual bandpass sampling techniques. References will be made throughout the rest of this chapter to this material: in particular, Eq (9) will be referenced with the development of each bandpass sampling technique.

Bandpass sampling involves the uniform sampling of the bandpass signal by one or more train of impulses. In each case, equations for the bandpass signal will be developed in terms of its uniform samples. The minimum possible sampling

rates and the conditions for the minimum sampling rates will also be developed.

The purpose of this chapter is to develop these bandpass sampling techniques. Techniques are compared in Chapter III.

Direct Sampling

Introduction. Direct sampling will be developed from two points of view: the conventional approach, referred to simply as direct sampling, is developed using an intuitive approach to give a "feel" for bandpass sampling theory; the second approach, called first-order sampling, is mathematically developed and reduces the sampling problem to an application of the low-pass sampling theorem.

Conventional Direct Sampling. The first bandpass sampling technique, direct sampling, can be viewed as the result of the product of a signal, $x(t)$, and a periodic pulse train, $p(t)$, just as in the case of low-pass sampling. The bandpass signal and the sampling process are demonstrated in Figure 15. Recall, when sampling bandpass waveforms we no longer have just one spectrum which is periodically replicated; instead, referring back to Figure 15b, there is a positive and a negative spectrum which get replicated. The sampled spectrum of the negative frequency portion of $X(\omega)$, $X_-(\omega)$, is sketched in Figure 15d, and corresponds to a periodic shift every $2\pi f_s$ rad/s. Similarly, the sampled spectrum of the positive frequency

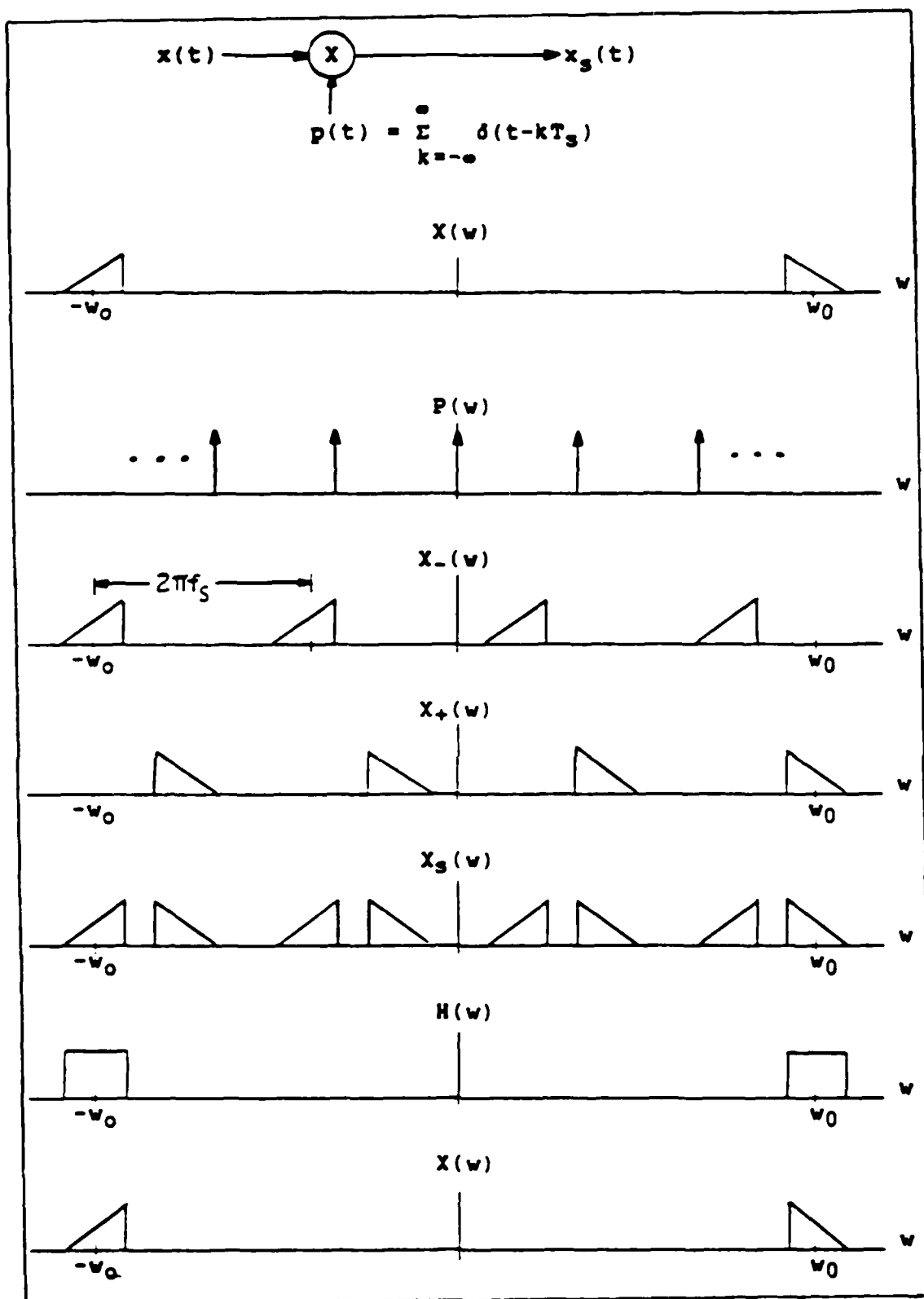


Figure 15. Bandpass Sampling Process (4:95)

portion of $X(\omega)$, $X_+(\omega)$, is sketched in Figure 15e. Figure 15f shows the combined result of the positive and negative spectrums being replicated. Reconstruction of $X(\omega)$ will be obtained by ideal bandpass filtering of $X_s(\omega)$ over the original bandwidth of $X(\omega)$ as long as the sampling rate is such that none of the spectral replicas overlap in the original bandpass region.

Analysis. A closer examination of the sampled spectrum provides insight in determining the minimum sampling rate possible. It will be shown that the Nyquist sampling rate for a bandpass waveform of twice the bandwidth, or σ/π samples/s, can be realized only when the signal is positioned in such a way that the upper cutoff frequency ($\omega_0 + \sigma/2$) is an integer multiple of σ . Otherwise the required sampling rate will be a value between σ/π and $2\sigma/\pi$ samples/s. To determine the minimum sampling rate for these two cases we'll consider each separately.

First, consider Case 1 in Figure 16 where $\omega_0 + \sigma/2 = k\sigma$ ($k = \text{integer}$). Just as we reconstructed the low-pass waveform in our earlier examples, we wish to be able to reconstruct our sampled waveform over the original bandpass spectrum. Notice in the Case 1, where $\omega_0 + \sigma/2 = k\sigma$ and $f_s = \sigma/\pi$ samples/s, none of the replicated spectrums overlap the original bandpass spectrum. Ideal bandpass filtering will recover our original bandpass waveform. This is not true in Case 2 of Figure 16. Here, the upper cutoff

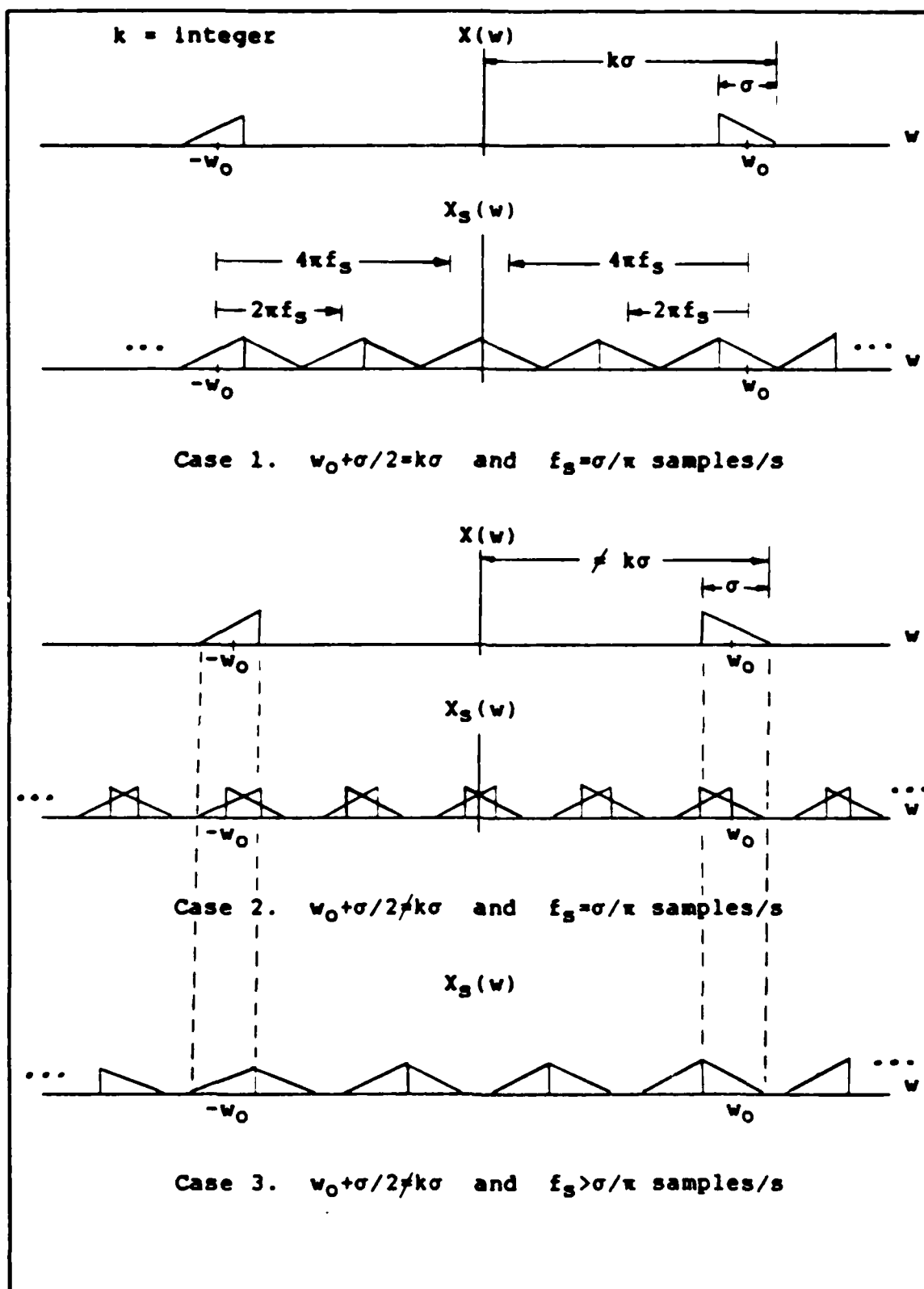


Figure 16. Direct Sampling - f_s for Three Different Cases

frequency is not an integer multiple of σ and if $f_s = \sigma/\pi$ samples/s as in Case 1, the shifted spectrums overlap within the original bandpass spectrum and there is aliasing. Ideal bandpass filtering will not recover our original signal. A higher sampling rate is needed to "adjust" the spectra until there is no overlapping spectra as in Case 3 for $\sigma/\pi < f_s < 2\sigma/\pi$ samples/s.

As stated before, the sampling frequency needed to prevent this aliasing will be somewhere between σ/π and $2\sigma/\pi$ samples/s. But how do you determine the actual sampling rate required? Refer to Figure 17, assume that the negative frequency spectrum of $X(\omega)$ is shifted just to the left of the positive frequency spectrum for some integer m , the $(m+1)$ integer shift must move it completely to the right to avoid overlap. In other words, we require that

$$(-\omega_0 + \sigma/2) + m2\pi f_s < \omega_0 - \sigma/2 \quad (25)$$

$$m\omega_s < 2\omega_0 - \sigma \quad (26)$$

$$\omega_s < (2\omega_0 - \sigma)/m \quad (27)$$

and

$$(-\omega_0 + \sigma/2) + (m+1)2\pi f_s > \omega_0 + \sigma/2 \quad (28)$$

$$(m+1)\omega_s > 2\omega_0 \quad (29)$$

$$\omega_s > (2\omega_0)/(m+1) \quad (30)$$

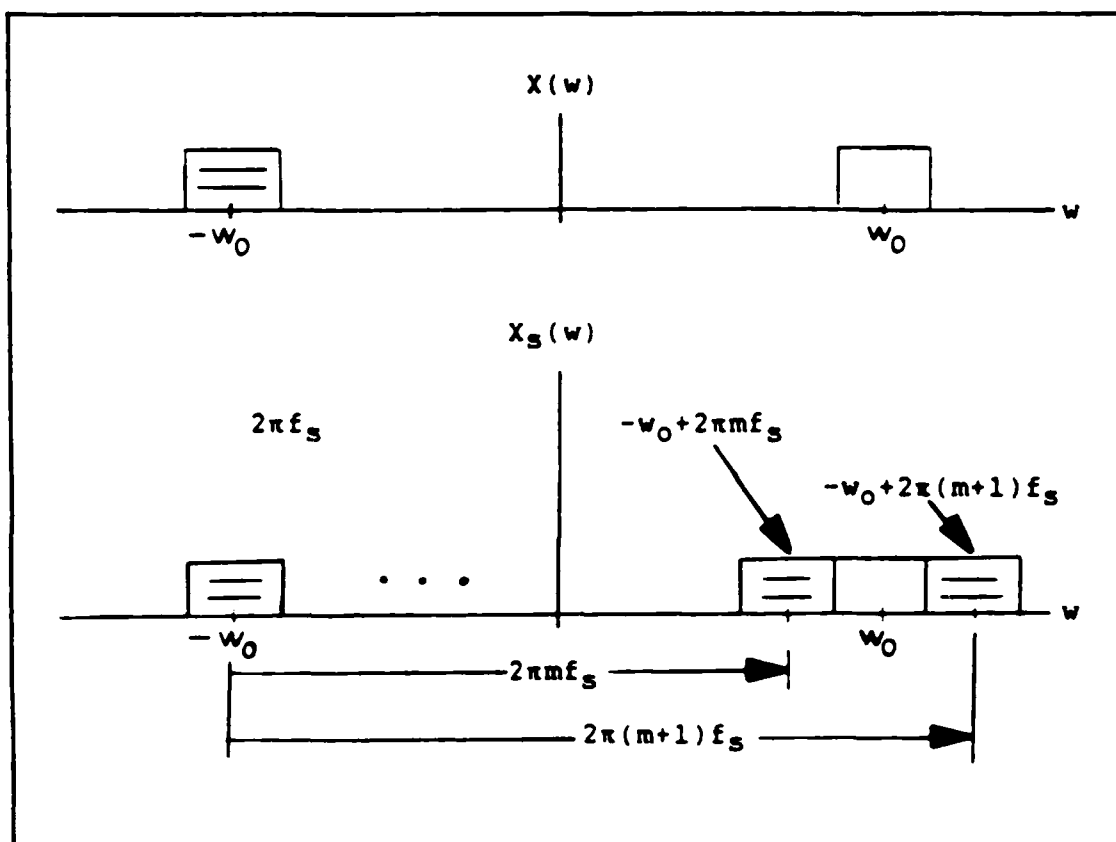


Figure 17. Determining $f_s(\min)$ (6:237-238)

or

$$(2w_0)/(m+1) < w_s < (2w_0 - \sigma)/m \quad (31)$$

From this, $w_s(\min)$ can be determined and w_s can be plotted.

Let

$$M = [(w_0 - \sigma/2)/\sigma] \quad (32)$$

where $[]$ denotes the greatest integer function. From

Eq (31)

$$w_s = (2w_0 - \sigma)/M \quad (33)$$

$$w_s = (2w_0 - \sigma)/[(w_0 - \sigma/2)/\sigma] \quad (34)$$

Equation (34) is plotted in Figure 18 as a function of $(w_0 + \sigma/2)/\sigma$. Notice that when $(w_0 + \sigma/2)/\sigma = \text{integer}$, the sampling rate is always twice the bandwidth, or σ/π samples/s. When $(w_0 + \sigma/2)/\sigma$ does not equal an integer, w_s must be determined from Eq (34) or interpolated from Figure 18.

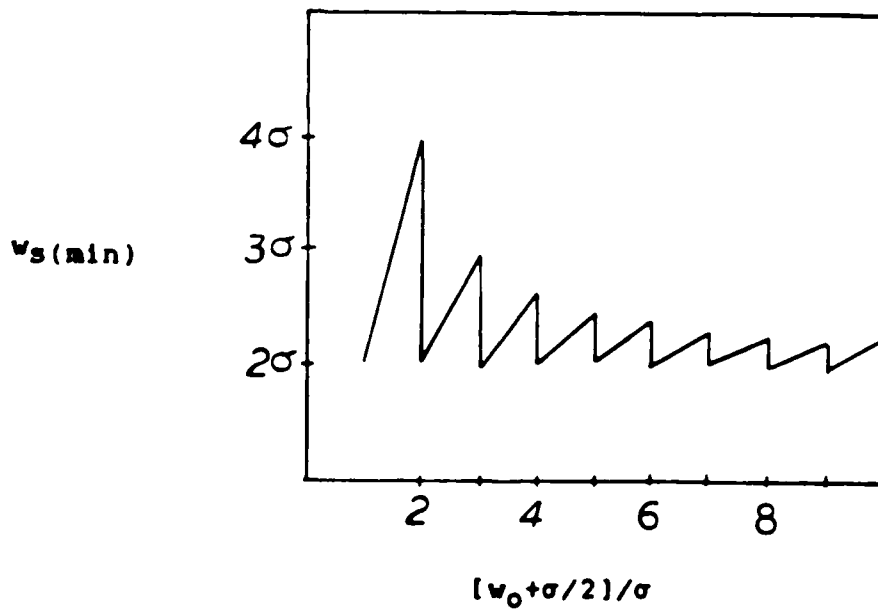


Figure 18. $w_s(\min)$ as a Function of w_0 and σ

Recall from our review of low-pass sampling that we found $x(t)$ in terms of its samples in Eq (9). That equation has the form

$$x(t) = \sum_{k=-\infty}^{\infty} x(kT_s)h(t-kT_s) \quad (9)$$

where T_s is the period between samples, $x(kT_s)$ are the samples, and $h(t)$ is the low-pass reconstruction filter, or the "interpolating function."

It is possible to extend Eq (9) to the case of a direct sampled bandpass signal. Since we want to reconstruct our sampled signal by ideal bandpass filtering over our original bandpass spectrum, we can use the transfer pair in Figure 19 and show that our bandpass filter $h(t)$ is

$$h(t) = (\sigma T_s / \pi) \text{Sa}(\sigma t / 4\pi) \cos \omega_0 t \quad (35)$$

where $\text{Sa}(x) = \sin x / x$, and $x(t)$, in terms of its uniform samples, becomes

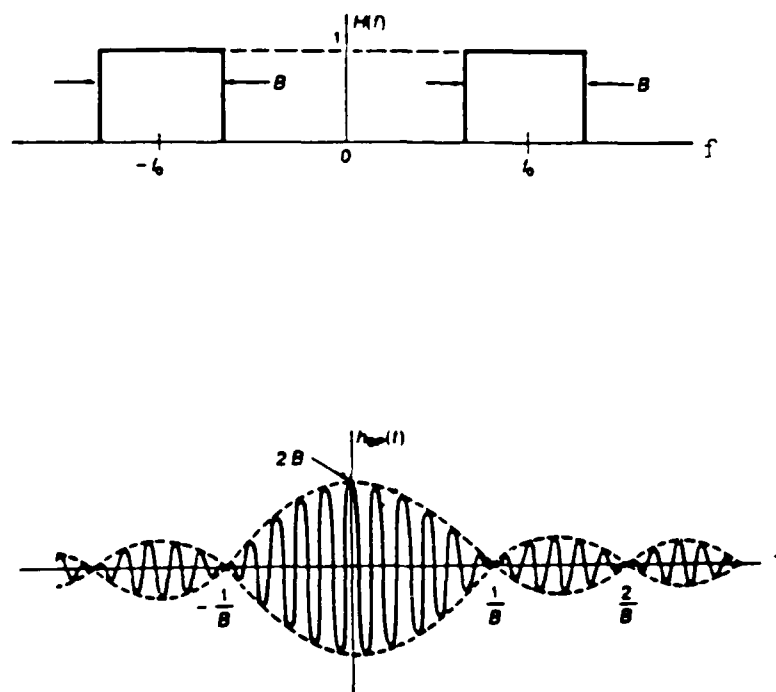
$$x(t) = (\sigma T_s / \pi) \sum_{k=-\infty}^{\infty} x(kT_s) \text{Sa}[\sigma(t-kT_s) / 4\pi] \cos[\omega_0(t-kT_s)] \quad (36)$$

This bandpass sampling theorem is constrained to the sampling rate in Figure 18 and Eq (34).

Note, from Figure 18, for narrowband systems where

$$\sigma \ll \omega_0 = \omega_0 + (\sigma/2) \quad (37)$$

it is possible to sample at the Nyquist rate and still



$$2B \text{sinc}(B\tau/2) \cos \omega_0 t$$

where $\sigma = 2\pi B$ and $\omega_0 = 2\pi f_0$

Figure 19. Bandpass Transfer Pair (4:,54,55,420)

recover the bandpass waveform.

The subject of direct bandpass sampling followed very closely the theory involved in low-pass sampling. Our bandlimited bandpass signal is sampled by multiplying it with a pulse train. For recovery, a window function (an ideal bandpass reconstruction filter) is applied to our properly sampled (f_s chosen to prevent aliasing) signal.

First-Order Sampling. An alternative approach to direct sampling, also called first-order sampling, was examined by John L. Brown (3:613-615). He showed that the first-order sampling of a bandpass signal is reduced to an application of the low-pass sampling theorem when the upper cutoff frequency is an integer multiple of the bandwidth. He uses a simple band-embedding technique to restore the positioning constraint when the upper cutoff frequency is not equal to an integer multiple of the bandwidth.

This proof uses only the standard quadrature representation of the bandpass signal and the classical sampling theorem for low-pass signals. For real numbers w_0, σ satisfying $w_0 \geq \sigma/2 > 0$ we define $\beta(w_0, \sigma)$ to consist of all complex valued bandpass signals x which can be represented in the form

$$x(t) = (1/2\pi) \int_{I_1, I_2} x(w) \exp(jwt) dw \quad \text{for all } t \quad (38)$$

where

$$I_1 = I_1(w_0, \sigma) \equiv (w_0 - \sigma/2, w_0 + \sigma/2) \quad (39)$$

$$I_2 = -I_1 \equiv (-w_0 - \sigma/2, -w_0 + \sigma/2) \quad (40)$$

and

$$\int_{I_1, I_2} |x(w)|^2 dw < \infty \quad (41)$$

thus x possesses finite energy and all its derivatives are continuous. If $w_0 + \sigma/2 = k\sigma$ for some positive integer k , then $x(t)$ can be represented by samples taken at an average rate of σ/π samples/s. If $(w_0 + \sigma/2)/\sigma$ is not an integer

(the general case), then the bandwidth σ is increased to σ' , where $(w_0 + \sigma/2)/\sigma' = [(w_0 + \sigma/2)/\sigma]$, and $[]$ denotes the greatest integer function. For the general case, an average sampling rate between σ/π and $2\sigma/\pi$ samples/s is needed.

Analysis. Let $x(t)$ be a bandpass signal having all its spectral components in the band $w_0 - (\sigma/2) \leq |w| \leq w_0 + (\sigma/2)$ so that (w_0, σ) characterizes the position of the band. Also, let $x \in \beta(w_0, \sigma)$.

Under these assumptions $x(t)$ may be represented as

$$x(t) = p(t)\cos w_0 t - q(t)\sin w_0 t \quad (42)$$

for all t , where $p(t)$ and $q(t)$ are low-pass functions

bandlimited to $|w| \leq \sigma/2$. Each of these signals, $p(t)$ and $q(t)$, may be sampled at a rate of $\sigma/2\pi$ samples/s.

This analysis is broken into two phases. In the first phase we assume $w_0 + \sigma/2 = k\sigma$, where k is a fixed positive integer and in the second phase (the general case) we assume $w_0 \geq \sigma/2 > 0$ (arbitrary band positioning).

Case 1. Where $x(t)$ is defined by Eq (42) and

$$x(nT) = p(nT)\cos(nw_0T) - q(nT)\sin(nw_0T) \quad (43)$$

Assume $T = \pi/\sigma$ corresponding to a sampling rate of σ/π samples/s. So,

$$x(nT) = p(nT)\cos(n\pi w_0/\sigma) - q(nT)\sin(n\pi w_0/\sigma) \quad (44)$$

and with $w_0 + \sigma/2 = k\sigma$, where k is fixed positive integer $\{w_0/\sigma = (k-1/2) = [(2k-1)/2]\}$

$$x(nT) = p(nT)\cos[n\pi(2k-1)/2] - q(nT)\sin[n\pi(2k-1)/2] \quad (45)$$

Where n is even, $n = 2v$, and letting $T_1 = 2T = 2\pi/\sigma$ the sine term goes to zero and

$$x(2vT) = x(2vT_1/2) = x(vT_1) = p(vT_1)(-1)^v \quad (46)$$

Where n is odd, $n = 2v-1$, the cosine term goes to zero and

$$x[(2v-1)T] = x[(2v-1)T_1/2] \quad (47)$$

$$x((2v-1)T_1/2) = x(vT_1 - T_1/2) = (-1)^{v+k+1} q(vT_1 - T_1/2) \quad (48)$$

Notice that the samples $\{p(vT_1)\}_{v=-\infty}^{\infty}$ determine $p(t)$ by the classical Shannon Theorem and the samples $\{q(vT_1 - T_1/2)\}_{v=-\infty}^{\infty}$ determine $q(t)$. The low-pass sampling expansions are

$$p(t) = \sum_{v=-\infty}^{\infty} p(vT_1) \phi_{\sigma}(t - vT_1) \quad (49)$$

$$q(t) = \sum_{v=-\infty}^{\infty} q(vT_1 - T_1/2) \phi_{\sigma}(t - vT_1 + T_1/2) \quad (50)$$

where

$$\phi_{\sigma}(t) = [\sin(\sigma t/2)]/(\sigma t/2) \quad (51)$$

Plugging in Eqs (49) and (50) into Eq (42)

$$\begin{aligned} x(t) = & \sum_{v=-\infty}^{\infty} p(vT_1) \phi_{\sigma}(t - vT_1) \cos \omega_0 t \\ & - \sum_{v=-\infty}^{\infty} q(vT_1 - T_1/2) \phi_{\sigma}(t - vT_1 + T_1/2) \sin \omega_0 t \end{aligned} \quad (52)$$

Let $T_1 = 2T$

$$\begin{aligned}
 x(t) = & \sum_{v=-\infty}^{\infty} p(2vT) \phi_{\sigma}(t-2vT) \cos w_0 t \\
 & - \sum_{v=-\infty}^{\infty} q(2vT-T) \phi_{\sigma}(t-2vT+T) \sin w_0 t \quad (53)
 \end{aligned}$$

but from Eq (46)

$$p(2vT) = x(2vT)(-1)^v \quad (54)$$

and from Eq (48)

$$q(2vT-T) = x[(2v-1)T](-1)^{v+k} \quad (55)$$

Plugging these into Eq (53)

$$\begin{aligned}
 x(t) = & \sum_{v=-\infty}^{\infty} x(2vT)(-1)^v \phi_{\sigma}(t-2vT) \cos w_0 t \\
 & - \sum_{v=-\infty}^{\infty} x[(2v-1)T](-1)^{v+k} \phi_{\sigma}(t-2vT+T) \sin w_0 t \quad (56)
 \end{aligned}$$

Now, letting $v = n$

$$\begin{aligned}
 x(t) = & \sum_{n=-\infty}^{\infty} x(2nT)(-1)^n \phi_{\sigma}(t-2nT) \cos w_0 t \\
 & - \sum_{n=-\infty}^{\infty} x[(2n-1)T](-1)^{n+k} \phi_{\sigma}(t-2nT+T) \sin w_0 t \quad (57)
 \end{aligned}$$

Since $w_0 t = (2k-1)\pi/2$

$$\cos w_0 t = \cos w_0 (t-2nT) \quad (58)$$

and since

$$(-1)^{n+k} \sin w_0 t = \cos w_0 [-(2n-1)T] \quad (59)$$

Eq (57) becomes

$$x(t) = \sum_{-\infty}^{\infty} x(vT) \phi_{\sigma}(t-vT) \cos w_0(t-vT) \quad (60)$$

which is the desired form of the expression for the case $w_0 + \sigma/2 = k\sigma$.

Case ii. For the general case, we assume arbitrary band position and $w_0 \geq \sigma/2 > 0$. Define

$$r = [(w_0 + \sigma/2)/\sigma] \quad (61)$$

with

$$r \leq (w_0 + \sigma/2)/\sigma < r+1 \quad (62)$$

Holding the upper cutoff frequency, $w_0 + \sigma/2$, constant (Figure 20) and increasing the bandwidth σ to σ' such that $(w_0 + \sigma/2)/\sigma' = r$.

Now,

$$w_0' = (w_0 + \sigma/2) - \sigma'/2 \quad (63)$$

$$I_1(w_0', \sigma') > I_1(w_0, \sigma) \quad (64)$$

$$I_2(w_0', \sigma') > I_2(w_0, \sigma) \quad (65)$$

and $x \in \beta(w_0', \sigma')$

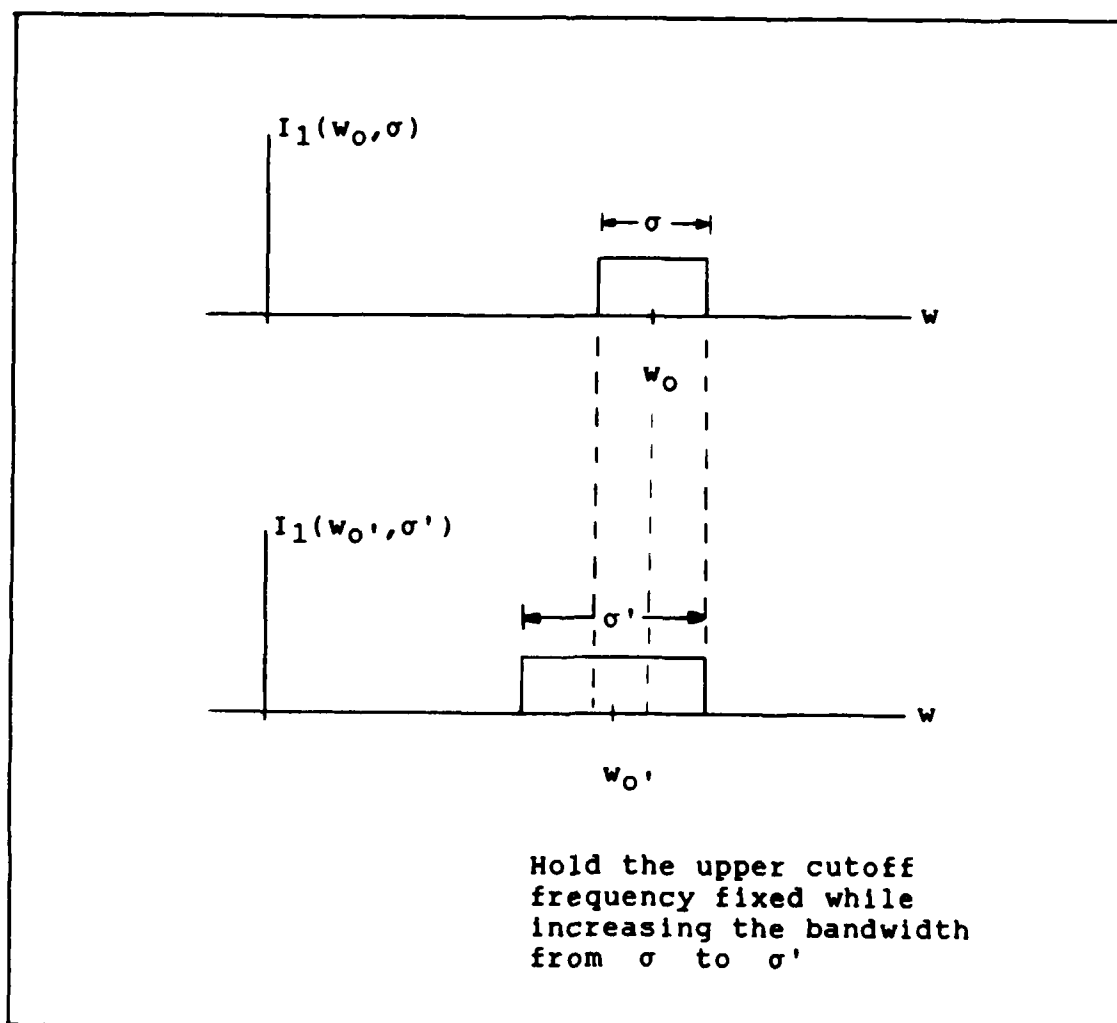


Figure 20. Embedding Technique for First-Order Sampling

The upper cutoff frequency $w_0 + \sigma/2$ is a multiple of σ' and σ , T , and w_0 are replaced in Eq (60) by σ' , $T' = \pi/\sigma'$, and w_0' respectively.

We now have

$$x(t) = x(nT') \Phi_{\sigma'}(t - nT') \cos w_0'(t - nT') \quad (66)$$

So a representation of $x(t)$ is possible with uniform samples at a rate of

$$f_s = 1/T' = \sigma'/\pi = \alpha\sigma/[\alpha]\pi \quad (67)$$

samples/s where $\alpha = (w_0 + \sigma/2)/\sigma$

Summary. Uniform sampling of a bandpass signal at an average rate of σ/π samples/s will suffice to determine the signal for all values of time only when the upper cutoff frequency is an integer multiple of the bandwidth. For the case where the upper cutoff frequency is not an integer multiple of the bandwidth, an average rate between σ/π and $2\sigma/\pi$ samples/s is required. For direct sampling, this rate can be determined from Eq (34) or from Figure 18. For first-order sampling, Brown demonstrated a simple band embedding technique which can be used to determine the minimum sampling rate for the signal. Brown's approach used only the quadrature representation of the bandpass signal and the classical Shannon sampling theorem in his proofs. The sampling rate, f_s , for the general case is given by Eq (67).

pth-order Sampling

Introduction. Kohlenberg extended the idea of first-order sampling to pth-order sampling (8:1432-1436). Unlike first-order sampling which involves a single train of uniformly separated samples of the bandpass waveform, pth-order sampling involves p trains of samples. The trains are

slightly displaced in time but occur at the same frequency (10:40).

The following development discusses pth-order sampling followed by second-order sampling (the case where $p = 2$). To date, only quadrature sampling, a special case of second-order sampling, has been shown to be a practical approach to pth-order bandpass sampling. For that reason, quadrature sampling will be covered in greater detail.

The second-order development will lead to a representation of $x(t)$ in terms of its uniform samples just as in the previous developments; however, in this case, $x(t)$ will be represented by two trains of uniform samples.

pth-Order Sampling Analysis. (8:1442-1443) Kohlenberg considered the spectra of amplitude modulated sequences of pulses of the form

$$g(t) = \sum_{n=-\infty}^{\infty} x(an)s(t-an) \quad (68)$$

where

$s(t)$ gives the shape of the basic pulse, and

$x(t)$ represents the modulating amplitude

Here, the function $g(t)$ represents the first-order sampling. Kohlenberg defined pth-order sampling as a function

$$g(t) = \sum_{i=1}^p g_i(t) \quad (69)$$

$$g(t) = \sum_{i=1}^p \left\{ \sum_{n=-\infty}^{\infty} x(a_i n + k_i) s_i(t - a_i n - k_i) \right\} \quad (70)$$

where the i th sampling of $g_i(t)$ has step size a_i , phase k_i , and sampling function $s_i(t)$.

To find the Fourier transform of $g(t)$ consider

$$g_i(t) = \sum_{n=-\infty}^{\infty} x(a_i n + k_i) s_i(t - a_i n - k_i) \quad (71)$$

Using the Dirac, δ , function this becomes

$$g_i(t) = \sum_{n=-\infty}^{\infty} \int_{-\infty}^{+\infty} x(\gamma) s_i(t - \gamma) \delta(\gamma - a_i n - k_i) d\gamma \quad (72)$$

Interchanging the order of summation and integration

$$g_i(t) = \int_{-\infty}^{+\infty} x(\gamma) s_i(t - \gamma) \left\{ \sum_{n=-\infty}^{\infty} \delta(\gamma - a_i n - k_i) \right\} d\gamma \quad (73)$$

This summation in brackets represents a periodic function with period a_i . Using its Fourier-series expansion

$$\sum_{n=-\infty}^{\infty} \delta(\gamma - a_i n - k_i) = \sum_{n=-\infty}^{\infty} a_i^{-1} \exp\{j2\pi n(\gamma - k_i)/a_i\} \quad (74)$$

and rewriting

$$g_i(t) = \int_{-\infty}^{+\infty} x(\gamma) s_i(t - \gamma) a_i^{-1} \left\{ \sum_{n=-\infty}^{\infty} \exp\{j2\pi n(\gamma - k_i)/a_i\} d\gamma \right\} \quad (75)$$

$$g_i(t) = a_i^{-1} \sum_{n=-\infty}^{\infty} \left\{ \int_{-\infty}^{+\infty} s_i(t-\gamma) x(\gamma) \exp(j2\pi n\gamma/a_i) d\gamma \exp(-j2\pi nk_i/a_i) \right\} \quad (76)$$

Taking the Fourier transform (F.T.) of both sides of this equation and using the fact that

$$\text{F. T.}\{x(\gamma) \exp(j2\pi n\gamma/a_i)\} = X(w+2\pi n/a_i) \quad (77)$$

$$G_i(w) = a_i^{-1} \sum_{n=-\infty}^{\infty} \exp(-j2\pi nk_i/a_i) S_i(w) X(w+2\pi n/a_i) \quad (78)$$

Summing over all "i" yields

$$G(w) = \sum_{i=1}^p a_i^{-1} S_i(w) \left\{ \sum_{n=-\infty}^{\infty} X(w+2\pi n/a_i) \exp(-j2\pi nk_i/a_i) \right\} \quad (79)$$

This pth-order sampling theorem gives the Fourier transform of $g(t)$ in terms of the sampled function $x(t)$ and the sampling parameters.

Second-Order Sampling Analysis. (13:907) Second-order sampling is a specialized case of pth-order sampling ($p=2$). Two equally effective implementations of second-order sampling are pictured in Figure 21. In one case the bandpass signal is passed through two channels, one channel is delayed in time and both channels are then simultaneously sampled. In the other implementation, the bandpass signal is once again fed through two channels; however, this time one of the sample trains is delayed (Figure 22). The samples occur at the same frequency but are delayed in time from each other.

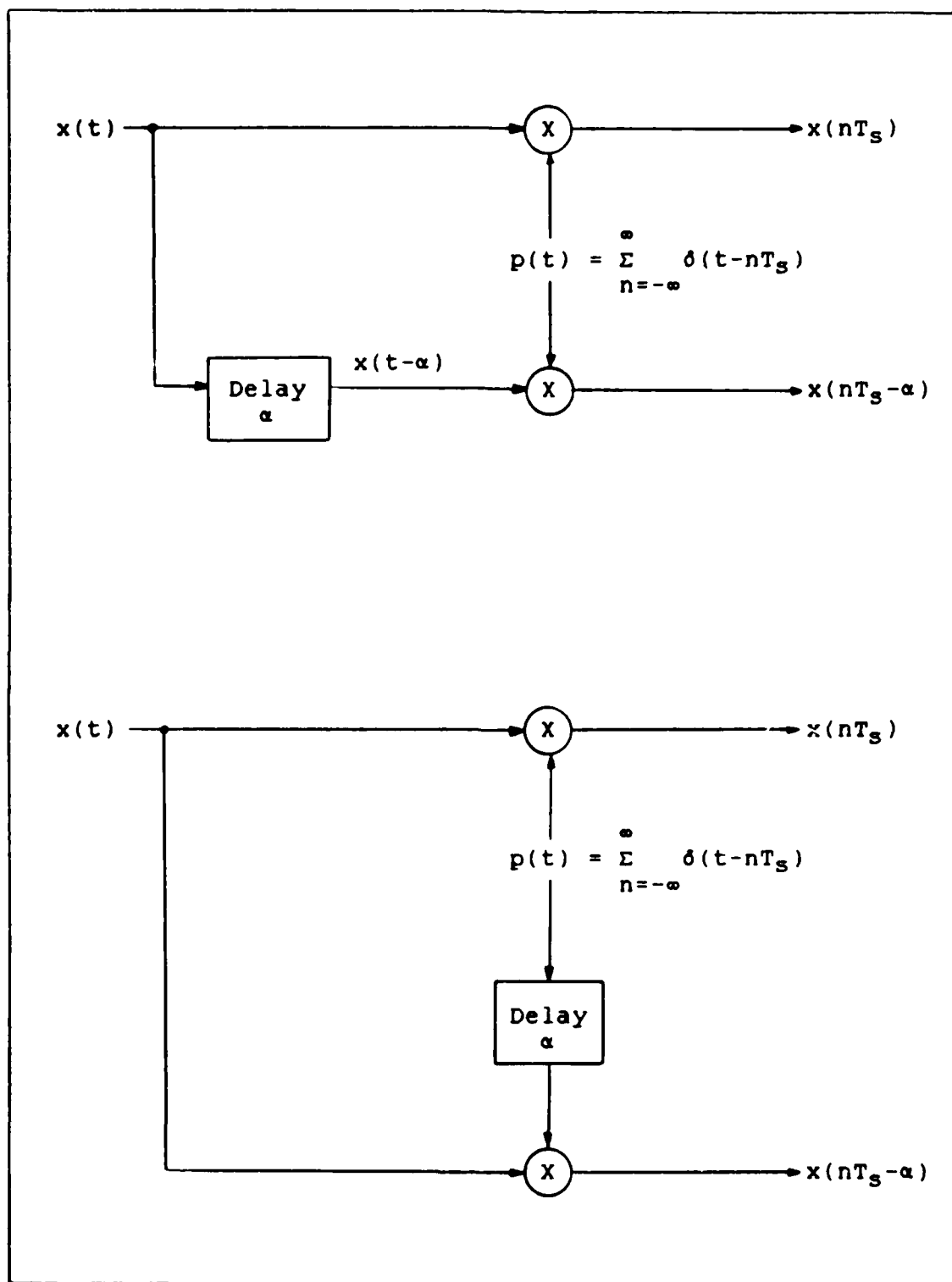


Figure 21. Second-Order Sampling (13:905)

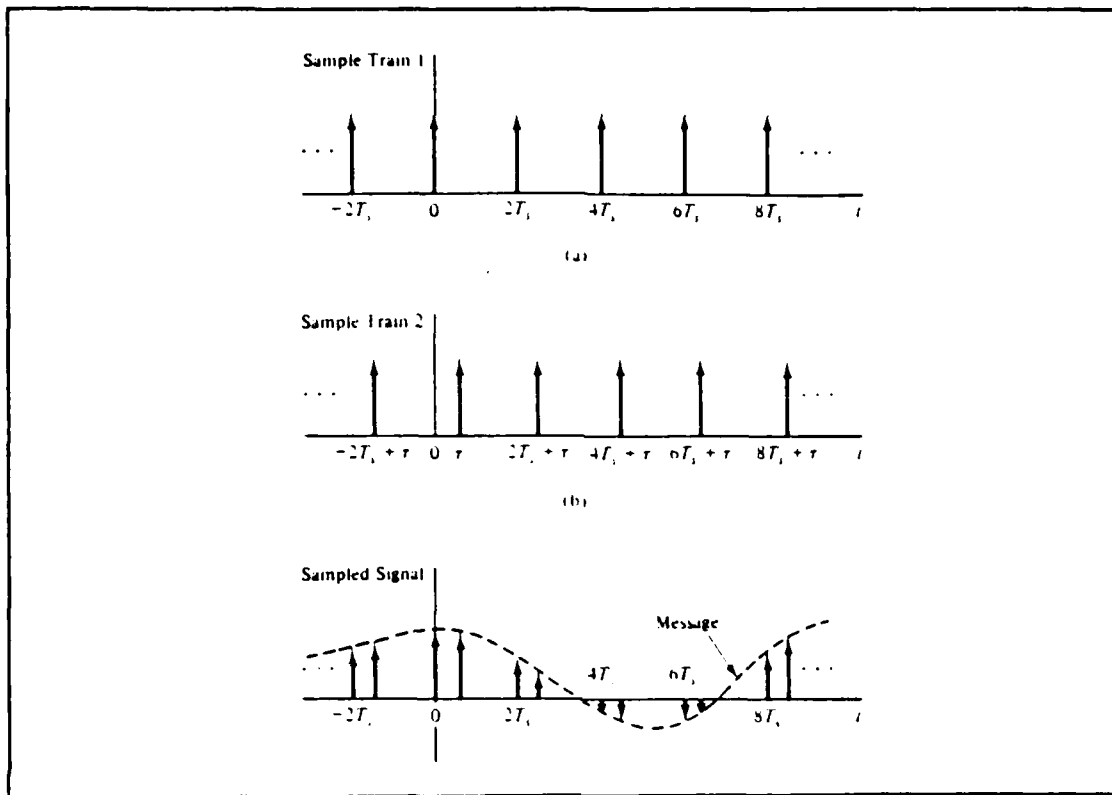


Figure 22. Sample Trains For Second-Order Sampling (10:41)

As mentioned, second-order sampling yields two sets of uniformly spaced samples which are interleaved, i.e.,

$$x_1(mT) = x(mT) \quad (80)$$

and

$$x_2(mT) = x(mT - \alpha) \quad (81)$$

where T is the temporal offset of the staggered sequence.

The sequence $x_1(mT)$ has the Fourier transform given by

$$X_1(\omega) = X(\omega) \quad (82)$$

and the transform of $x_2(mT)$ is

$$X_2(w) = (1/T) \sum_{m=-\infty}^{\infty} X(w+2\pi m/T) \exp\{-j[w+(2\pi m/T)]\alpha\} \quad (83)$$

The use of $x_2(mT)$ introduces a new degree of freedom over first-order sampling which can be used to eliminate aliasing.

The original waveform can be recovered by properly filtering and combining the two sequences, i.e.,

$$x(t) = \sum_{m=-\infty}^{\infty} x_1(mT)h_D(t-mT) + \sum_{m=-\infty}^{\infty} x_2(mT)h_D(-t+mT-\alpha) \quad (84)$$

For exact reconstruction an ideal bandpass filter is required with frequency transfer characteristics, $H_D(w)$ given by

$$H_D(w) = \begin{cases} 0, & 0 \leq w \leq w_0 - (\pi/T) \\ A_1, & w_0 - (\pi/T) \leq w \leq \{2\pi[(2k-1)/2]/T\} - w_0 \\ A_2, & \{2\pi[(2k-1)/2]/T\} - w_0 \leq w \leq w_0 + (\pi/T) \\ 0, & w_0 + (\pi/T) \leq w \leq 2\pi/T \end{cases} \quad (85)$$

where

$$A_1 = \{\exp\{-j[(2k-1)/2]\beta - \pi/2\}\} / (2/T) \sin\{[(2k-1)/2]\beta\} \quad (86)$$

$$A_2 = \{\exp[-j(k\beta - \pi/2)]\} / (2/T) \sin(k\beta) \quad (87)$$

$$\beta = 2\pi\alpha/T \quad (88)$$

and k is the largest integer for which

$$\lfloor (k-1)/T \rfloor < f_0 - (1/2T) \quad (89)$$

Conventional Quadrature Sampling

Introduction. As mentioned in Chapter I, it is possible to preprocess a signal prior to sampling to insure being able to sample at the Nyquist rate. Recall, that a bandpass signal can be represented in the form

$$x(t) = p(t)\cos\omega_0 t - q(t)\sin\omega_0 t \quad (42)$$

where $p(t)$ and $q(t)$, the in-phase and quadrature components, respectively, are low-pass signals with spectra occupying the symmetric band $|w| \leq \sigma/2$; effectively, the bandpass signal is specified by a pair of low-pass signals.

The objective of conventional quadrature sampling is to recover the low-pass components, $p(t)$ and $q(t)$, and to sample them at the Nyquist rate. Because of the preprocessing of $x(t)$, the low-pass components are independent and may be sampled independently (10:36). This means that there is only the Nyquist limit to satisfy. We no longer have to be concerned with two bandpass spectrums overlapping or the relationship between the upper cutoff frequency and the bandwidth. Samples of the low-pass components will uniquely determine our original bandpass signal.

Analysis. A common approach to obtaining the quadrature components is to employ quadrature demodulation

as shown in Figure 23 (13:907-908). In one channel $x(t)$ is modulated by $\cos w_0 t$, or

$$x(t)\cos w_0 t = [p(t)\cos w_0 t - q(t)\sin w_0 t]\cos w_0 t \quad (90)$$

$$x(t)\cos w_0 t = p(t)\cos^2 w_0 t - q(t)\sin w_0 t \cos w_0 t \quad (91)$$

Recall,

$$\cos^2 A = 1/2 + (1/2)\cos 2A \quad (92)$$

$$\sin A \cos B = (1/2)[\sin(A+B) + \sin(A-B)] \quad (93)$$

Here $A = B$, so

$$\sin A \cos A = (1/2)\sin 2A \quad (94)$$

$$x(t)\cos w_0 t = (1/2)[p(t) + p(t)\cos 2w_0 t - q(t)\sin 2w_0 t] \quad (95)$$

The filter removes the $2w_0$ terms, and

$$x(t)\cos w_0 t \approx p(t)/2 \quad (96)$$

Similarly, $q(t)$ is obtained from the sine channel.

$$x(t)\sin w_0 t = p(t)\sin w_0 t \cos w_0 t - q(t)\sin^2 w_0 t \quad (97)$$

$$\sin^2 w_0 t = (1/2)[1 - \cos 2w_0 t] \quad (98)$$

$$x(t)\sin w_0 t = (1/2)[p(t)\sin 2w_0 t - q(t) + q(t)\cos 2w_0 t] \quad (99)$$

Once again, filtering out the $2w_0$ terms

$$x(t)\sin w_0 t \approx -q(t)/2 \quad (100)$$

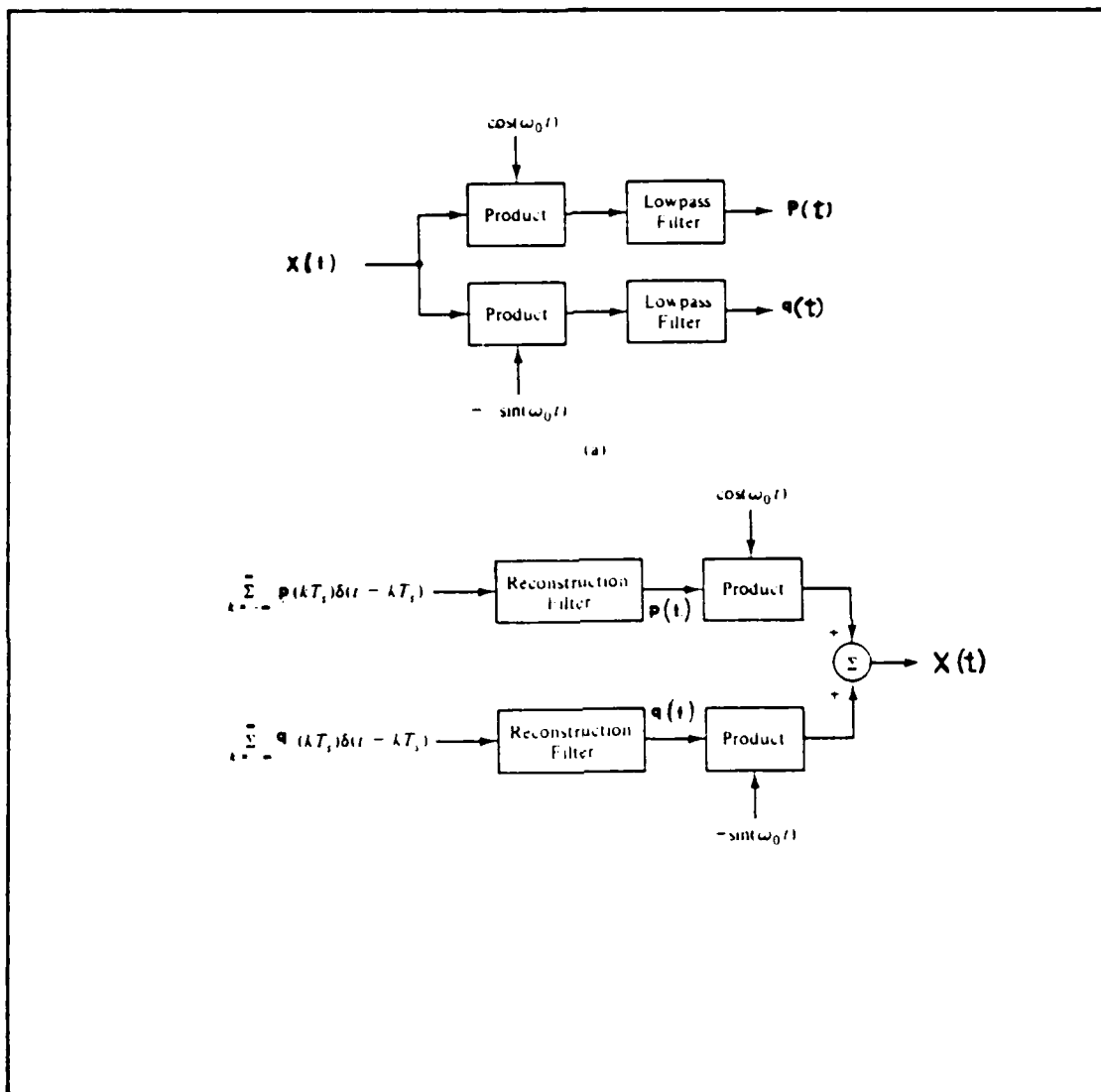


Figure 23. Conventional Quadrature Sampling (10:37)

Both channels are then sampled at a rate of $\sigma/2\pi$ samples/s. The samples are written as

$$p(t) = \sum_{k=-\infty}^{\infty} p(kT_s) \delta(t - kT_s) \quad (101)$$

$$q(t) = \sum_{k=-\infty}^{\infty} q(kT_s) \delta(t - kT_s) \quad (102)$$

These equations have the familiar form of a low-pass signal in terms of its samples. The next step in the process is to apply the samples to the reconstruction filters as in Figure 23b. These reconstruction filters are the spectral windows referenced earlier. Signals $p(t)$ and $q(t)$ are modulated once again to yield the familiar form of Eq (42)

$$x(t) = p(t) \cos \omega_0 t - q(t) \sin \omega_0 t \quad (42)$$

Summary. Conventional quadrature sampling allows us to sample an arbitrary bandlimited bandpass signal at a total rate of σ/π samples/s, using preprocessing, regardless of the ratio of the center frequency and the bandwidth, and recover $x(t)$.

Quadrature Sampling

Introduction. This approach to quadrature sampling is illustrated in Figure 24. Instead of preprocessing to determine the low-pass components, $p(t)$ and $q(t)$ are determined from samples of the bandpass signal and its quarter-wavelength extension (7:1453-1454).

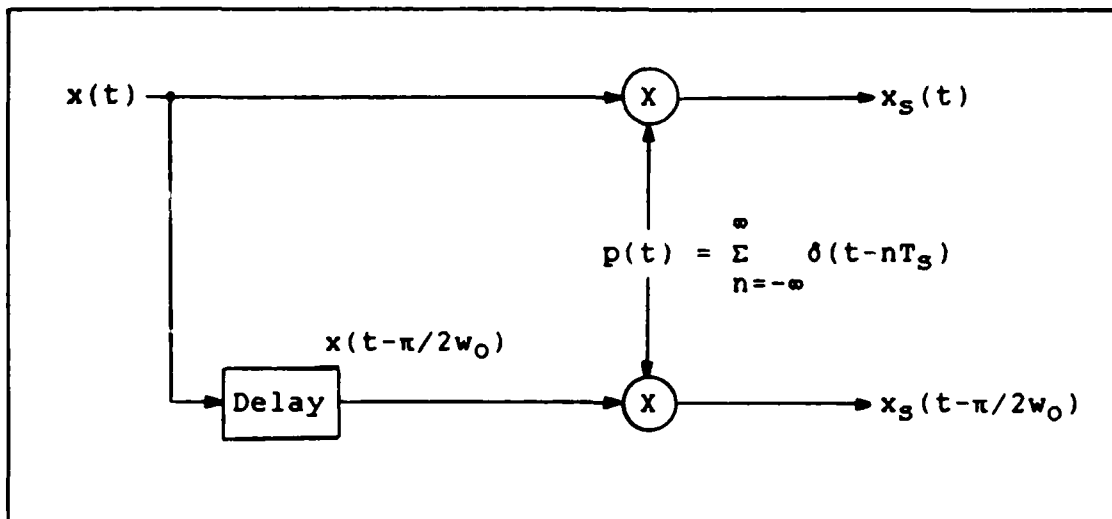


Figure 24. Quadrature Sampling

Three cases will be discussed. In Case i it is assumed that $2\omega_0/\sigma = k$, where k is an integer ≥ 1 . It will be shown that sampling at an average rate of σ/π samples is sufficient to recover the bandpass signal. Case ii assumes only that $0 < \sigma/2 \leq \omega_0 < \infty$; i.e., $2\omega_0/\sigma$ may or may not equal k . A technique is applied where $I_1(\omega_0, \sigma)$ is embedded in a larger band, $I_1(\omega_0, \sigma')$, having the same center frequency ω_0 , and a bandwidth $\sigma' \geq \sigma$. In Case iii, $I_1(\omega_0, \sigma)$ is embedded in an "optimal" band, $I_1(\omega_0', \sigma')$, that requires $2\omega_0'/\sigma'$ to be an integer. Cases ii and iii allow sampling at an average rate between σ/π and $2\sigma/\pi$ samples/s as will be explained in detail in the following paragraphs.

Case i. (2:1660) Quadrature sampling's goal is to recover the low-pass components $p(t)$ and $q(t)$ directly from samples taken of the bandpass signal $x(t)$ and its

quarter-wavelength translation $x(t-\pi/2w_0)$ (2:1659). Case 1 assumes the constraint $2w_0/\sigma = k$, where k is an integer ≥ 1 .

Recalling Eq (42)

$$x(t) = p(t)\cos w_0 t - q(t)\sin w_0 t \quad (42)$$

In terms of its samples $x(t)$ becomes

$$x(nT_1) = p(nT_1)\cos(nw_0T_1) - q(nT_1)\sin(nw_0T_1) \quad (103)$$

Letting $T_1 \equiv 2\pi/\sigma$ and $2w_0/\sigma = k$

$$\begin{aligned} x(nT_1) &= p(nT_1)\cos\{n(\sigma k/2)(2\pi/\sigma)\} \\ &\quad - q(nT_1)\sin\{n(\sigma k/2)(2\pi/\sigma)\} \end{aligned} \quad (104)$$

$$x(nT_1) = p(nT_1)\cos(n\pi k) - q(nT_1)\sin(n\pi k) \quad (105)$$

or,

$$x(nT_1) = (-1)^{kn} p(nT_1) \quad (106)$$

$$x(nT_1 - \pi/2w_0) = (-1)^{kn} q(nT_1 - \pi/2w_0) \quad (107)$$

These equations show that samples of $p(t)$ at a rate of $1/T_1 = \sigma/2\pi$ samples/s are available from the original bandpass waveform $x(t)$, as are samples of $q(t-\pi/2w_0)$ at $\sigma/2\pi$ samples/s. Recall that $p(t)$ and $q(t)$ are bandlimited to $|w| \leq \sigma/2$, which implies that they can be reconstructed from their samples at the low-pass rate.

From the Shannon low-pass sampling theorem

$$p(t) = \sum_{n=-\infty}^{\infty} p(nT_1)\phi(t-nT_1) \quad (108)$$

where

$$\phi(t) = \{\sin(\sigma t/2)\}/(\sigma t/2) \quad (109)$$

So, plugging Eq (106) into Eq (108) yields

$$p(t) = \sum_{n=-\infty}^{\infty} (-1)^{kn} x(nT_1)\phi(t-nT_1) \quad (110)$$

Similarly,

$$q(t-\alpha) = \sum_{n=-\infty}^{\infty} q(nT_1-\alpha)\phi(t-nT_1) \quad (111)$$

where α is real.

Let $t = t + \alpha$

$$q(t) = \sum_{n=-\infty}^{\infty} q(nT_1-\alpha)\phi(t+\alpha-nT_1) \quad (112)$$

For $\alpha = \pi/2w_0$

$$q(t) = \sum_{n=-\infty}^{\infty} q(nT_1-\pi/2w_0)\phi\{t+(\pi/2w_0)-nT_1\} \quad (113)$$

Plugging Eq (107) into Eq (112)

$$q(t) = \sum_{n=-\infty}^{\infty} (-1)^{kn} x(nT_1-\pi/2w_0)\phi\{t+(\pi/2w_0)-nT_1\} \quad (114)$$

So, by plugging Eqs (110) and (113) into Eq (42)

$$\begin{aligned}
 x(t) = & \sum_{n=-\infty}^{\infty} (-1)^{kn} x(nT_1) \phi(t-nT_1) \cos w_0 t \\
 & - \sum_{n=-\infty}^{\infty} (-1)^{kn} x(nT_1 - \pi/2w_0) \phi\{t + (\pi/2w_0) - nT_1\} \sin w_0 t \quad (115)
 \end{aligned}$$

which is the desired quadrature sampling formula for the case $2w_0/\sigma = k = \text{integer} \geq 1$.

The low-pass components $p(t)$ and $q(t)$ were sampled at a rate of $\sigma/2\pi$ samples/s yielding an average rate of σ/π samples/s for the bandpass signal.

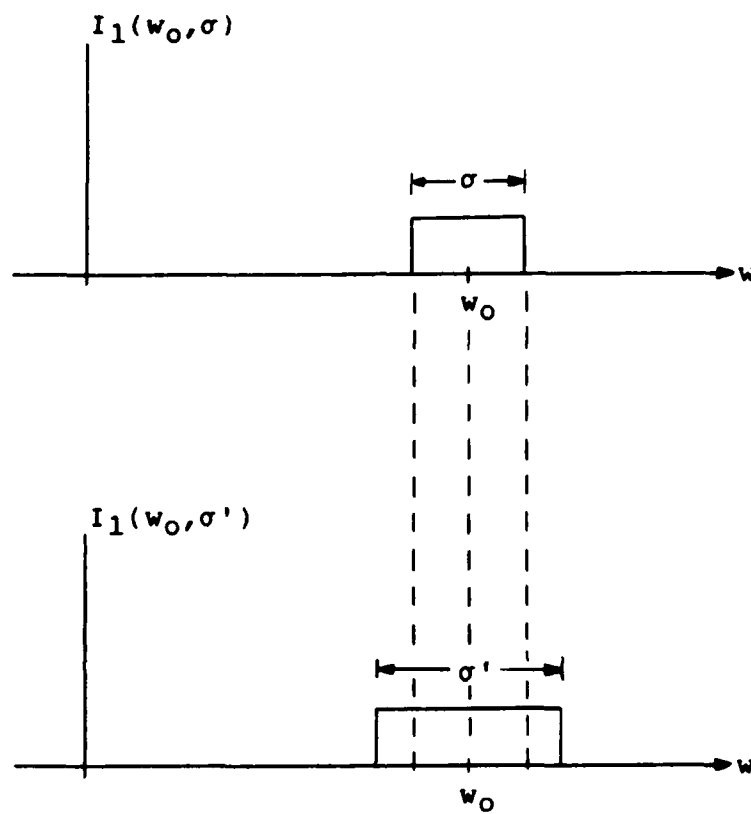
Case ii. (2:1660) For this case assume only that $w_0 > w_0 \geq \sigma/2 > 0$. In other words, $2w_0/\sigma$ need not always be an integer. Here $I_1(w_0, \sigma)$ is embedded in a larger band $I_1(w_0, \sigma')$ which has the same center frequency and a bandwidth $\sigma' \geq \sigma$ as shown in Figure 25. Holding w_0 constant, and increasing σ (if necessary) to the value σ' such that $2w_0/\sigma'$ will be an integer, yields

$$2w_0/\sigma' = [2w_0/\sigma] = s = \text{integer} \quad (116)$$

where

$$s \leq 2w_0/\sigma < s+1 \quad (117)$$

The results of Case i now apply with σ , T_1 , k , replaced with σ' , $T_1' = 2\pi/\sigma'$, s respectively. So,



Hold the center
frequency fixed while
increasing the bandwidth
from σ to σ'

Figure 25. Embedding Technique - Case 11

$$p(t) = \sum_{n=-\infty}^{\infty} (-1)^{Sn} x(nT_1') \phi_1(t - nT_1') \quad (118)$$

$$q(t) = \sum_{n=-\infty}^{\infty} (-1)^{Sn} x(nT_1' - \pi/2w_0) \phi_1\{t + (\pi/2w_0) - nT_1'\} \quad (119)$$

where

$$\phi_1(t) \equiv \{\sin(\sigma't/2)\}/(\sigma't/2) \quad (120)$$

Sampling $x(t)$ and $x(t - \pi/2w_0)$ at the rate

$$1/T_1' = \sigma'/2\pi = \{(2w_0/\sigma)/[2w_0/\sigma]\}(\sigma/2\pi) \quad (121)$$

or

$$1/T_1' = \{2\alpha/[2\alpha]\}(\sigma/2\pi) \quad (122)$$

yields an average sampling rate

$$(2\alpha/[2\alpha])(\sigma/\pi) \quad (123)$$

samples/s for the reconstruction of $x(t)$ from Eq (42)

$$x(t) = p(t)\cos w_0 t - q(t)\sin w_0 t \quad (42)$$

When $2w_0/\sigma$ is an integer Eq (123) becomes σ/π samples/s, which is the equivalent to Case 1 as expected.

Case iii. (2:1661) In this case it is not necessary to hold w_0 or σ fixed. Here, $x(t)$ is a general bandpass signal, w_0 doesn't have a strict sense of center (angular) frequency, but only a sense of "average of extremes" ($w_0 - \sigma/2$ and $w_0 + \sigma/2$).

Again, assume that $\omega > \omega_0 \geq \sigma/2 > 0$, and that $2\omega_0/\sigma$ may or may not equal an integer. The objective is to determine a generalized result by allowing another degree of freedom in the embedding technique of Case 11.

For this embedding technique, the upper cutoff frequency, $\omega_0 + \sigma/2$, is held invariant while increasing the bandwidth (Figure 26). An "optimal" covering band $I_1(\omega_0', \sigma'')$ is determined where it is required that $2\omega_0'/\sigma'' =$ integer. The analysis follows.

Let $s = [2\omega_0/\sigma]$ be the greatest integer contained in $2\omega_0/\sigma$ and $s \leq 2\omega_0/\sigma < s+1$. From Figure 26, it is obvious that

$$\omega_0' = (\omega_0 + \sigma/2) - \sigma''/2 \quad (124)$$

where $\sigma'' \geq \sigma$

To determine σ'' , set

$$2\omega_0'/\sigma'' = 2\{\omega_0 + (\sigma/2) - \sigma''/2\}/\sigma'' = s = [2\omega_0/\sigma] \quad (125)$$

or

$$2\omega_0'/\sigma'' = (2\omega_0 + \sigma - \sigma'')/\sigma'' = s = [2\omega_0/\sigma] \quad (126)$$

Solving for σ''

$$\sigma''s = 2\omega_0 + \sigma - \sigma'' \quad (127)$$

$$\sigma''s + \sigma'' = 2\omega_0 + \sigma \quad (128)$$

$$\sigma''(s+1) = 2\omega_0 + \sigma \quad (129)$$

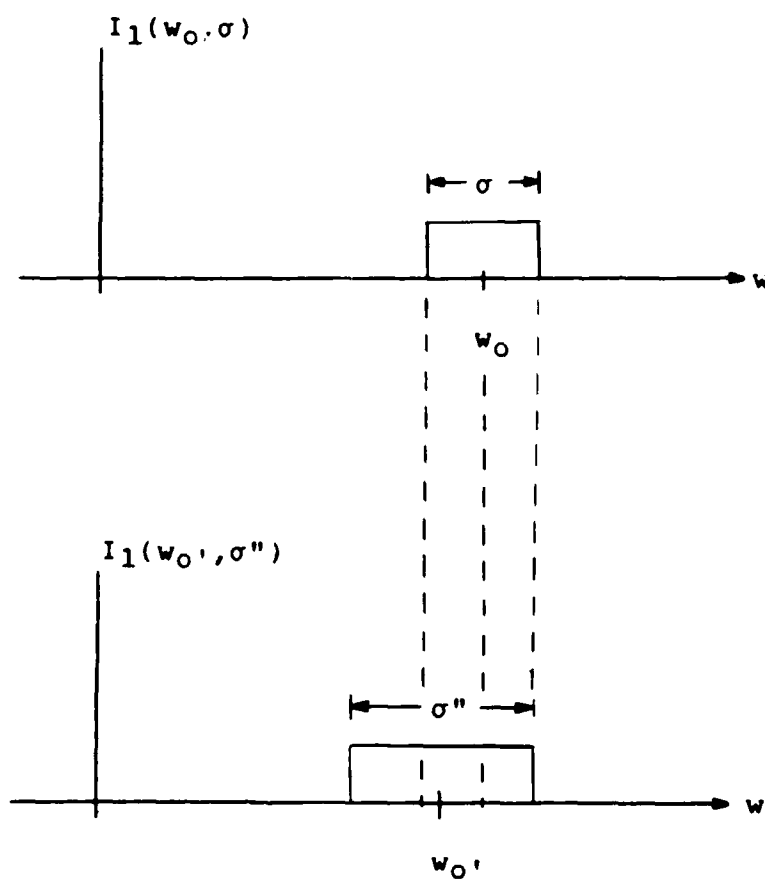


Figure 26. Embedding Technique - Case iii

$$\sigma'' = (2w_0 + \sigma)/(s+1) \quad (130)$$

$$\sigma'' = \{\sigma(2w_0/\sigma)+1\}/\{[2w_0/\sigma]+1\} \quad (131)$$

Now, let $\gamma = w_0/\sigma$

$$\sigma'' = \{\sigma(2\gamma+1)\}/[2\gamma+1] \quad (132)$$

If $\gamma \geq 1$ then $\sigma'' < 2\sigma$ and $w_0 - \sigma/2 < w_0' \leq w_0$.
Further, $w_0' + \sigma''/2 = w_0 + \sigma/2$; i.e., the upper cutoff frequency of the covering band remains invariant.

The low-pass components $p(t)$ and $q(t)$ with respect to the center frequency w_0' have the form

$$p(t) = \sum_{n=-\infty}^{\infty} (-1)^{sn} x(nT_1'') \phi_2(t - nT_1'') \quad (133)$$

$$q(t) = \sum_{n=-\infty}^{\infty} (-1)^{sn} x(nT_1'' - \pi/2w_0') \phi_2\{t + (\pi/2w_0') - nT_1''\} \quad (134)$$

where

$$\phi_2(t) \equiv \{\sin(\sigma''t/2)\}/(\sigma''t/2) \quad (135)$$

and

$$T_1'' = 2\pi/\sigma'' \quad (136)$$

With

$$x(t) = p(t)\cos w_0't - q(t)\sin w_0't \quad (136)$$

$$\begin{aligned}
x(t) = & \sum_{n=-\infty}^{\infty} (-1)^{S_n} x(nT_1'') \phi_2(t - nT_1'') \cos w_0' t \\
& - \sum_{n=-\infty}^{\infty} (-1)^{S_n} x(nT_1'' - \pi/2w_0') \phi_2\{t + (\pi/2w_0') - nT_1''\} \sin w_0' t
\end{aligned} \tag{138}$$

the average sampling rate in this reconstruction is

$$\{(2\gamma+1)/[2\gamma+1]\}(\sigma/\pi) \tag{139}$$

samples/s. Since

$$(2\gamma+1)/[2\gamma+1] \leq 2\gamma/[2\gamma] \tag{140}$$

the sampling rate is improved over that in Case ii.

Summary. In Case i an average sampling rate of σ/π samples/s was determined for the reconstruction of $x(t)$ from

$$x(t) = p(t) \cos w_0 t - q(t) \sin w_0 t \tag{42}$$

for the situation where the upper cutoff frequency was an integer multiple of the bandwidth. When this constraint doesn't hold, the average sampling rate was

$\{(2\gamma)/[2\gamma]\}(\sigma/\pi)$ samples/s as determined in Case ii. Since $1 \leq 2\gamma/[2\gamma] < 2$ for all $\gamma \geq 1/2$, the average rate necessary for reconstruction of $x(t)$ varies from σ/π to $\sigma/2\pi$ samples/s. Lastly, when the frequency w_0 is allowed to vary, a further improvement in the sampling rate can be obtained, the average rate being given by Eq (139).

Complex Sampling

Introduction. Another possibility for maintaining the (average) sampling rate equal to the minimum value of σ/π samples/s is to sample both $x(t)$ and its Hilbert transform at a rate of $1/T_s = \sigma/2\pi$ samples/s (10:37). Since $x(t)$ and its quadrature function are Hilbert transforms of each other, the low-pass components, $p(t)$ and $q(t)$, can once again be determined, this time from samples of $x(t)$ and its Hilbert transform, $x_H(t)$.

Analysis. (13:906) This technique, illustrated in Figure 27, is equivalent to forming the analytic signal

$$z_x(t) \equiv x(t) + jx_H(t) \quad (141)$$

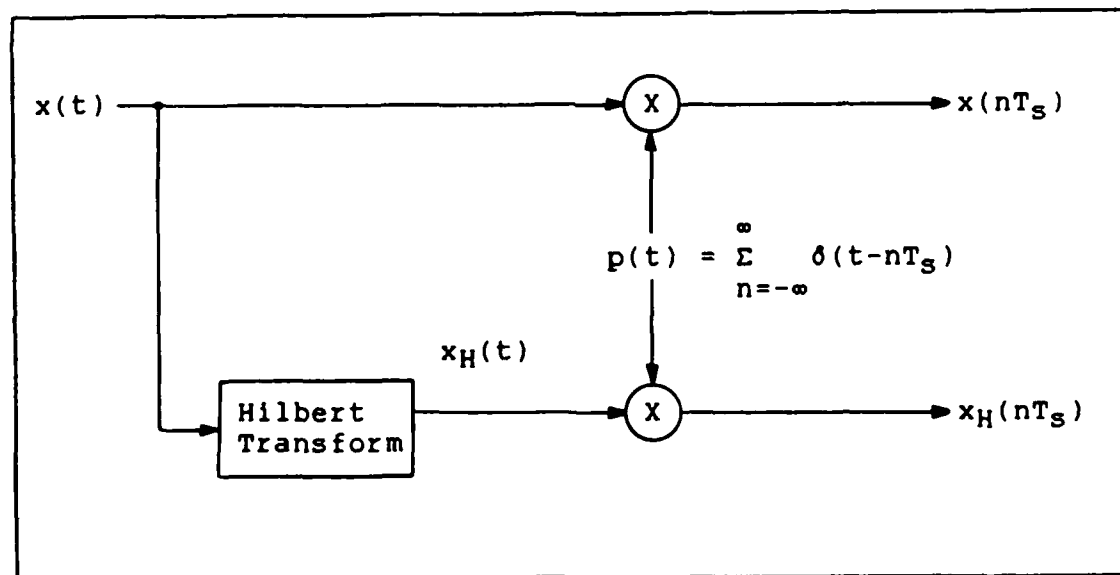


Figure 27. Complex Sampling (13:905)

The Hilbert transform of $x(t)$, $x_H(t)$, is obtained by the following operation

$$x_H(t) = -j\text{sgn}(\omega)X(\omega) \quad (142)$$

The Fourier transform of the analytic signal, $Z_X(t)$, is

$$Z_X(\omega) = \begin{cases} 2X(\omega), & \omega > 0 \\ X(\omega), & \omega = 0 \\ 0, & \omega < 0 \end{cases} \quad (143)$$

For the bandpass case, $X(0) = 0$ and $Z_X(t) = 2X(\omega)U(\omega)$, where U is the step function.

In terms of the positive and negative frequency spectra, $X_+(\omega)$ and $X_-(\omega)$, respectively, which are illustrated in Figure 28,

$$X(\omega) = X_+(\omega) + X_-(\omega) \quad (144)$$

where

$$X_+(\omega) = \begin{cases} X(\omega), & \omega \geq 0 \\ 0, & \text{otherwise} \end{cases} \quad (145)$$

$$X_-(\omega) = \begin{cases} X(\omega), & \omega \leq 0 \\ 0, & \text{otherwise} \end{cases} \quad (146)$$

Thus,

$$Z_X(\omega) = 2X_+(\omega) \quad (147)$$

The analytic signal

$$Z_X(t) = x(t) + jx_H(t) \quad (148)$$

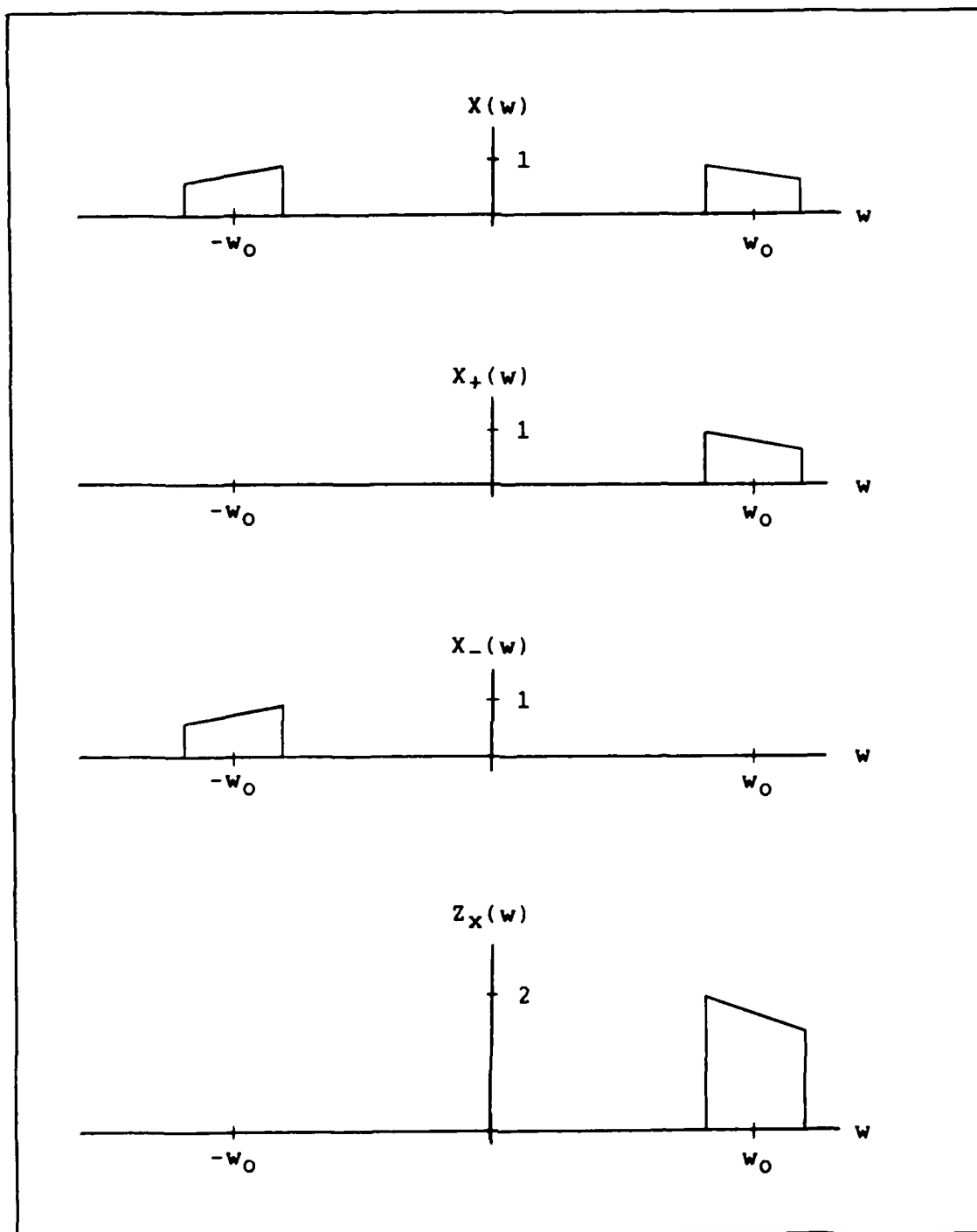


Figure 28. Fourier Transform of an Analytic Signal (13:907)

has a spectrum confined to the positive frequencies

$\omega_0 - \sigma/2 < \omega < \omega_0 + \sigma/2$. So we can write

$$Z_X(t) = \sum_{n=-\infty}^{\infty} Z_X(nT_S) \text{sinc}[\sigma(t-nT_S)/2] \exp[j\omega_0(t-nT_S)] \quad (149)$$

and from this,

$$x(t) = \text{Re}\{Z_X(t)\} \quad (150)$$

$$\begin{aligned} x(t) = \sum_{n=-\infty}^{\infty} \{ & x(nT_S) \text{sinc}[\sigma(t-nT_S)/2] \cos[\omega_0(t-nT_S)] \\ & - x_H(nT_S) \text{sinc}[\sigma(t-nT_S)/2] \sin[\omega_0(t-nT_S)] \} \end{aligned} \quad (151)$$

Once again we have the familiar form of Eq (42)

$$x(t) = p(t) \cos \omega_0 t - q(t) \sin \omega_0 t \quad (42)$$

Summary. Obviously there is not a strict separate interpolation in Eq (151) since the "carriers" are $\cos[\omega_0(t-nT_S)]$ and $\sin[\omega_0(t-nT_S)]$. But, once again, the bandpass signal is represented in terms of its uniform samples.

Chapter Summary

As mentioned in the introduction, the purpose of this chapter was to develop, theoretically, the bandpass sampling techniques. In each case, $x(t)$ was developed in terms of its uniform samples. In addition, the minimum sampling rate was developed for each technique.

III. Results

Introduction

One "figure of merit" for comparing bandpass sampling techniques is to compare the minimum sampling rate possible for each case. The following is a review of the key results of Chapter II.

Direct sampling can be accomplished at a minimum rate of $f_s = \sigma/\pi$ samples/s only when $\omega_0 + \sigma/2 = k\sigma$ ($k =$ integer). Otherwise, the minimum sampling rate is governed by the exact relationship between the bandwidth and the center frequency and can be determined from Eq (34) or from Figure 18.

For conventional quadrature sampling, the low-pass components can each be sampled at a minimum rate of $f_s = \sigma/2\pi$ samples/s for a total (average) rate of $f_s = \sigma/\pi$ samples/s. This approach allows arbitrary band positioning. In other words, the relationship between the center frequency and the bandwidth is not considered when determining the sampling rate. The preprocessing allows the low-pass components to be independently sampled according to the low-pass sampling theorem (10:36). Since we are usually interested in the amplitude, $A(t)$, and the phase, $\phi(t)$, of $x(t)$, the time-varying nature of our signal requires that samples of $p(t)$ and $q(t)$ be taken at the same instant (18:731).

Quadrature sampling allows sampling at the average rate

of $f_s = \sigma/\pi$ samples/s when $2w_0 = k\sigma$ ($k = \text{integer}$). Otherwise $f_s = \{(2\gamma+1)/(2\gamma+1)\}(\sigma/\pi)$ samples/s, where $\gamma = w_0/\sigma$. As in direct sampling, the minimum sampling rate is a function of the relationship between the center frequency and the bandwidth.

Another possibility for maintaining the (average) sampling rate equal to its minimum value σ/π samples/s in any case (arbitrary band position) is to sample both $x(t)$ and its Hilbert transform, $x_H(t)$, at a rate of $f_s = \sigma/2\pi$ samples/s.

The last three approaches offer a sampling rate reduction of up to one-half over direct sampling, but none of the approaches offer a significant rate reduction over each other. So, how do you choose a sampling scheme? The best answer to that question, ultimately, is determined by how the sampling scheme will fit into the overall system (receiver) design. There are many factors that must be considered when choosing a sampling scheme. For instance, if your design is being driven by cost, it may be cheaper to use a single A/D and use direct sampling. Or, using "off the shelf" equipment may keep the cost down and at the same time drive your design to match the available hardware. If the system design requires down-conversion, direct sampling or the conventional quadrature approach may be appropriate.

Since there is no real "figure of merit" to compare the individual sampling techniques (unless you base your

decision on the minimum sampling rate possible), selection of a sampling scheme should be made only after an examination of what it actually takes to implement these techniques in hardware.

A quick glance at the figures in Chapter I gives a pretty good idea of the hardware components needed, but there is more to consider. Recall in low-pass sampling, the theoretical minimum sampling rate was shown to be twice the highest frequency. That may be true in theory, but in practical applications the rate is higher. A good rule of thumb has been shown to be five times the highest frequency (14:53). The reason for the difference is that in the theoretical derivation all things were considered ideal. Signals had bandlimited spectrums and filters could pass or reject whatever frequencies were required. But the fact is, signals are not ideally bandlimited, and since bandpass sampling rates are typically determined based upon consideration of the bandwidth, some thought needs to be given to the definition of bandwidth. A few of the more popular definitions are given below (4:61-62).

Half-power bandwidth is the interval between the frequencies where the signal has dropped to half power (or 3 dB below the peak value).

The equivalent rectangular bandwidth is defined as the bandwidth which satisfies the relationship $P = W_n S(f_c)$, where P is the total signal power over all frequencies, W_n is the equivalent noise bandwidth, and $S(f_c)$ is the value of

the signal at the band center frequency (assumed to be the maximum value over all frequencies).

The null-to-null bandwidth is the width of the main spectral lobe, where most of the power is contained.

There are other definitions of bandwidth available, but the point is, there are many definitions of bandwidth and the definition you choose has a direct affect on the sampling rate, f_s .

Besides topics such as bandwidth, which effect each sampling scheme, there are other concerns that need to be addressed that are peculiar to the particular two-channel technique chosen. They will now be discussed.

Conventional Quadrature Sampling

Radar and communications systems are becoming increasingly dependent upon coherent digital processing. Conversion of signals from IF analog form into digital complex samples carrying amplitude and phase information has been traditionally implemented in the form of two parallel IF to baseband converters operated in quadrature each followed by A/D converters which thus provide digitized in-phase, $p(t)$, and quadrature, $q(t)$, components (conventional quadrature sampling - see Figure 23). Balancing the two baseband converters over a wide dynamic range is difficult and phase errors are typically 2° - 3° for commercial coherent detectors (18:731). To examine the effects of phase error in the quadrature sampling process, recall that any bandpass

waveform may be written

$$x(t) = p(t)\cos w_0 t - q(t)\sin w_0 t \quad (42)$$

Now, induce a phase error, θ , between the IF to baseband converters. In other words, assume we demodulate with $\cos w_0 t$ and $\sin(w_0 t + \theta)$. Beginning with the cosine channel

$$x(t)\cos w_0 t = [p(t)\cos w_0 t - q(t)\sin w_0 t]\cos w_0 t \quad (152)$$

$$x(t)\cos w_0 t = p(t)\cos^2 w_0 t - q(t)\sin w_0 t \cos w_0 t \quad (153)$$

$$x(t)\cos w_0 t = (1/2)[p(t) + p(t)\cos 2w_0 t - q(t)\sin 2w_0 t] \quad (154)$$

The low-pass filter removes the $2w_0$ terms, and

$$x(t)\cos w_0 t \approx (1/2)p(t) \quad (155)$$

Similarly, $q(t)$ is obtained from the sine channel.

$$\begin{aligned} x(t)\sin(w_0 t + \theta) &= p(t)\sin(w_0 t + \theta)\cos w_0 t \\ &\quad - q(t)\sin(w_0 t + \theta)\sin w_0 t \end{aligned} \quad (156)$$

But,

$$\sin A \cos B = (1/2)[\sin(A+B) + \sin(A-B)] \quad (157)$$

$$\sin A \sin B = (1/2)[\cos(A-B) - \cos(A+B)] \quad (158)$$

$$\begin{aligned} x(t)\sin(w_0 t + \theta) &= (1/2)p(t)[\sin(2w_0 t + \theta) + \sin \theta] \\ &\quad - (1/2)q(t)[\cos \theta - \cos(2w_0 t + \theta)] \end{aligned} \quad (159)$$

The low-pass filter removes the $2w_0$ terms, and

$$x(t)\sin(w_0 t + \theta) = (1/2)[p(t)\sin\theta - q(t)\cos\theta] \quad (160)$$

Normally we expect to be able to recover the amplitude, $A(t)$, and phase, $\phi(t)$, information about $x(t)$ using the following relations,

$$A(t) = [p^2(t) + q^2(t)]^{1/2} \quad (161)$$

$$\phi(t) = \tan^{-1}[p(t)/q(t)] \quad (162)$$

What we actually have is

$$A(t) \approx [p^2(t) + (p(t)\sin\theta)^2 + (q(t)\cos\theta)^2]^{1/2} \quad (163)$$

$$\phi(t) = \tan^{-1}\{p(t)/[p(t)\sin\theta - q(t)\cos\theta]\} \quad (164)$$

Obviously the phase error causes attenuation of the output signal. For small fixed errors, this is tolerable. For phase errors approaching $\pm 90^\circ$, however, the received signal is wiped out (17:206).

A further cause of concern, with the same consequences, is phase errors between the transmitter and the receiver. Typically, this is no major problem when the transmitter and receiver are in close proximity. Again, 2° - 3° is tolerable.

The key point to this discussion is that random phase errors must be controlled or the phase errors will render this conventional quadrature sampling approach useless.

Quadrature Sampling

NOTE: The material in this section parallels and expands on

Persons' quadrature sampling error formula (11:511-512). For that reason and ease of reference, Persons' notation will be used. To be consistent with the rest of this thesis we let $2\pi f_0 = \omega_0$ and $2\pi W = \sigma$.

Recall that the aim of quadrature sampling is to recover the low-pass components, $p(t)$ and $q(t)$, directly from samples of both the bandpass signal $x(t)$ and its quarter-wavelength translation $x(t-1/(4f_0))$, the samples being taken at the low-pass rate. The Grace-Pitt interpolation formula (7:1454).

$$g(t) = \sum_{n=-\infty}^{\infty} f(n/f_s) s(t-n/f_s) + \sum_{n=-\infty}^{\infty} f(n/f_s + 1/x f_0) s(t-n/f_s - 1/x f_0) \quad (165)$$

where $x = 4$, allows an exact reconstruction of high frequency bandlimited waveforms with a minimum average sampling rate of W samples/s (or $W/2$ samples/s/channel) whenever $2f_0 = kW$ as in Figure 29. This was verified by Persons when he developed a quadrature sampling error formula.

For the general case, where $2f_0$ does not equal kW , the interpolation formula given by Eq (165) with $x = 4$ will not exactly yield $f(t)$. Persons showed a way to measure the amount of reconstruction error when using this equation for the general case. More specifically, he determined Q , the

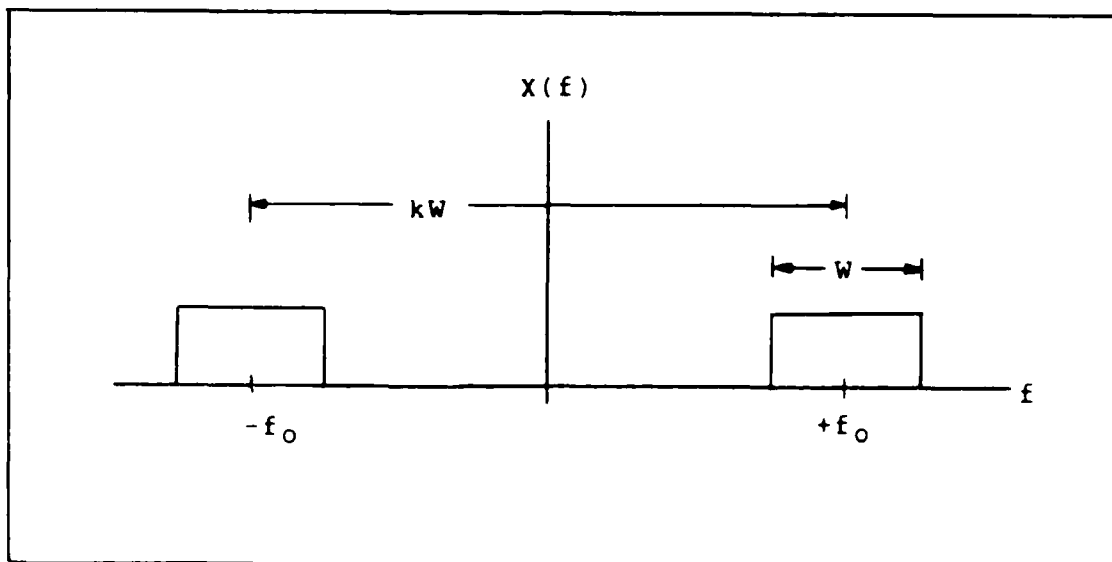


Figure 29. Bandpass Signal for $2f_0 = kW$ ($k = \text{integer}$)

ratio of the power in the error band to the power in the signal band.

By following the same approach taken by Persons, it is possible to more fully develop the quadrature sampling error formula into a generalized formula in which the effects on Q due to hardware timing errors can be investigated.

It will be shown that timing is extremely critical when sampling at or near $f_s = \sigma/\pi$ samples/s (average).

Analysis. Beginning with the general interpolation formula of Eq (165), recall that the objective is to determine the power in the error relative to the power in $f(t)$.

We can express Eq (165)

$$g(t) = [f(t) \sum_{n=-\infty}^{\infty} \delta(t-n/f_s)] * s(t)$$

$$+ [f(t) \sum_{n=-\infty}^{\infty} \delta(t-n/f_s - 1/x f_0)] * s(t) \quad (166)$$

where * denotes convolution.

Taking the Fourier transform of Eq (166) yields

$$G(f) = f_s S(f) \{ F(f) * [\sum_{n=-\infty}^{\infty} \delta(f-nf_s) + \sum_{n=-\infty}^{\infty} \delta(f-nf_s) \exp(-j2\pi n f_s / x f_0)] \} \quad (167)$$

$$G(f) = 2f_s S(f) \{ F(f) + (1/2) \sum_{n \neq 0} F(f-nf_s) [1 + \exp(-j2\pi n f_s / x f_0)] \} \quad (168)$$

Let $2f_s S(f) = 1$ in the region where $F(f)$ is nonzero and zero elsewhere,

$$2f_s S(f) = \{ \text{rect}[(f-f_0)/W] + \text{rect}[(f+f_0)/W] \} \quad (169)$$

This is equivalent to applying an ideal antialiasing filter to the bandpass signal. Solving for $S(f)$

$$S(f) = (1/2f_s) \{ \text{rect}[(f-f_0)/W] + \text{rect}[(f+f_0)/W] \} \quad (170)$$

The inverse Fourier transform of $S(f)$ is

$$s(t) = (W/f_s) \text{sinc}(Wt) \cos(2\pi f_0 t) \quad (171)$$

Substituting Eq (170) into Eq (168) yields

$$G(f) = F(f) + \{(1/2)\{\text{rect}[(f-f_0)/W] + \text{rect}[(f+f_0)/W]\}$$

$$\sum_{n \neq 0} F(n-nf_s)[1+\exp(-z\pi 2nf_s/xf_0)] \quad (172)$$

Notice that $G(f)$ is made up of $F(f)$, the term we want, plus some extra terms. It is the power in these extra terms relative to that in $F(f)$ that will be determined. Because of the rect functions (antialiasing filter), only the terms giving bands in the vicinity of f_0 will interfere.

Let $2f_0/f_s = z + x = K$, where $z = \text{integer}$. Also, assume that $f_s > W$, which is an obvious need or else the repeated spectral bands would overlap. Note that for $2f_0/f_s = z = \text{integer}$, and $x = 0$, there is only one band for $n = \pm z$ which overlaps $F(f)$, but the amplitude term $1 + \exp(-zx) = 0$. In general, there will be two bands overlapping $F(f)$, corresponding to the terms $n = \pm z, \pm(z+1)$. Considering only the positive frequencies, Figure 30 shows the z and $(z+1)$ terms overlapping $F(f)$ for the general case where $2f_0$ is not equal to kW ($k = \text{integer}$), and $f_s = W$ samples/s.

Define Q equal to the ratio of power in the extra bands to the power in $F(f)$, and again consider only positive frequencies.

Define

$$a_z = (1/2)[1 + \exp(-j\pi 4f_0 z/x 2f_0)] \quad (173)$$

$$a_{(z+1)} = (1/2)[1 + \exp(-j\pi 4f_0 (z+1)/x 2f_0)] \quad (174)$$

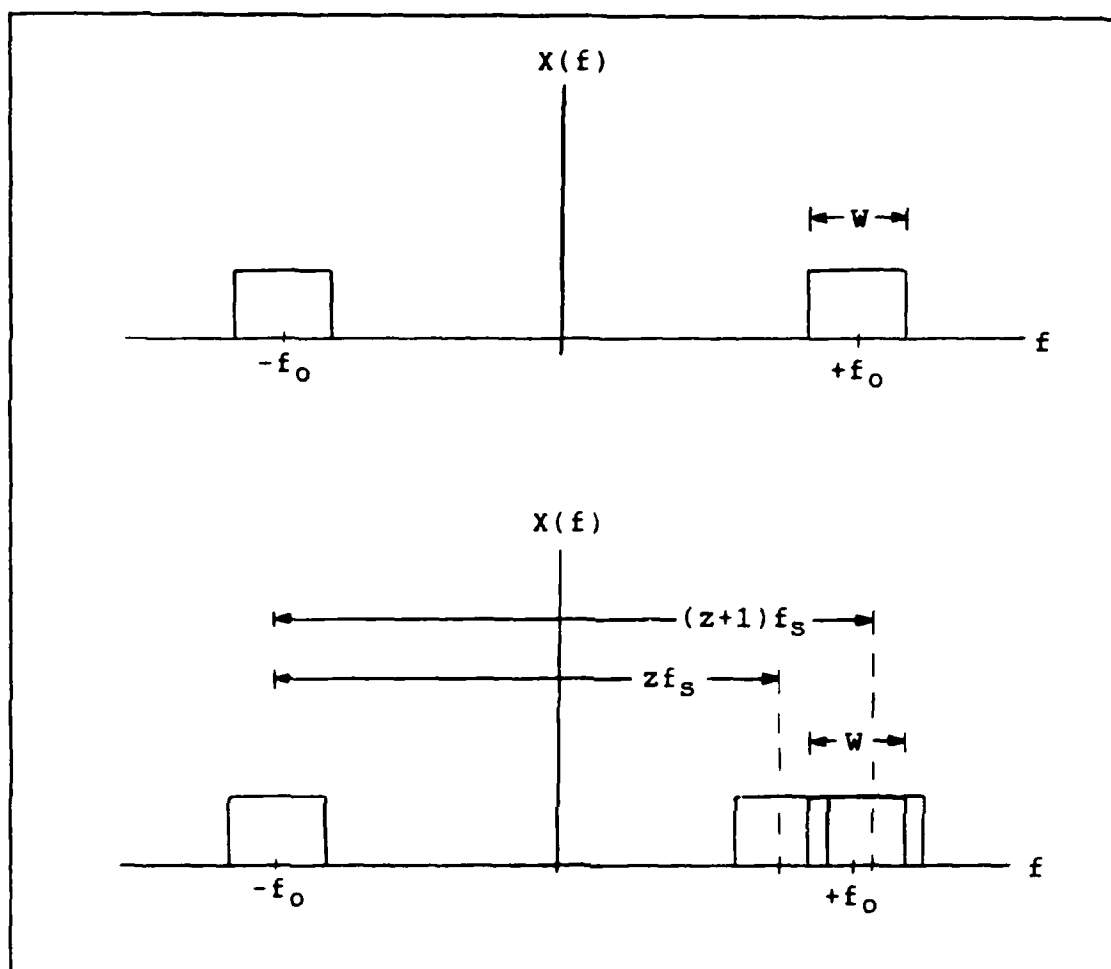


Figure 30. Bandpass Signal for $2f_0 \neq kW$ ($k = \text{integer}$)

$$B_z = \text{bandwidth of } z\text{th term} \quad (175)$$

$$B_{(z+1)} = \text{bandwidth of } (z+1)\text{st term} \quad (176)$$

Since we've applied the antialiasing filter, the numbers B_z and $B_{(z+1)}$ are determined by the overlap with $\text{rect}((f-f_0)/W)$. Let the power in $F(f) = W$; then from Eqs (172-176)

$$Q = |a_z|^2 (B_z/W) + |a_{(z+1)}|^2 [B_{(z+1)}/W] \quad (177)$$

where B_z and $B_{(z+1)}$ must be greater than zero, else they are taken as zero.

Now, from Eq (173)

$$|a_z|^2 = (1/4) |1 + \exp(-j\pi 4f_s z/x2f_0)|^2 \quad (178)$$

but $K = 2f_0/f_s$ and $z = [K]$, where $[]$ is the greatest integer function.

$$|a_z|^2 = (1/4) |1 + \exp(-j\pi 4[K]/xK)|^2 \quad (179)$$

$$|a_z|^2 = \{\cos^2(2\pi[K]/xK)\} \quad (180)$$

Likewise,

$$|a_{(z+1)}|^2 = (1/4) |1 + \exp\{-j\pi 4([K]+1)/xK\}|^2 \quad (181)$$

$$|a_{(z+1)}|^2 = \{\cos^2\{2\pi([K]+1)/xK\}\} \quad (182)$$

Note from Figure 30, the center of the z th band is at

$$f_z = \{zf_s - f_0\} = \{[K]2f_0/K - f_0\} \quad (183)$$

and the center of the $(z+1)$ st band is at

$$f_{(z+1)} = \{(z+1)f_s - f_0\} = \{([K]+1)2f_0/K - f_0\} \quad (184)$$

Now determine B_z/W . From Figure 30, $B_z = f_z + W - f_0$

So,

$$B_z/W = (f_z + W - f_o)/W \quad (185)$$

$$B_z/W = f_z/W + 1 - f_o/W \quad (186)$$

$$B_z/W = f_z/W + 1/2 - (f_o/W - 1/2) \quad (187)$$

Substituting

$$f_z = [K]2f_o/K - f_o \quad (188)$$

$$B_z/W = \{[K]2f_o/K - f_o\}/W + 1/2 - \{f_o/W - 1/2\} \quad (189)$$

Since $f_o = f_s K/2$; $K = 2f_o/f_s$

$$B_z/W = 1 - \{f_s(K-[K])\}/W \quad (190)$$

Likewise,

$$B_{(z+1)}/W = 1 - \{f_s(1-K+[K])\}/W \quad (191)$$

Substituting into Eq (177) and using the definition

$K = z + r = [K] + r$ and $L = f_s/W$

$$\begin{aligned} Q(K,L) = & \{\cos^2(2\pi[K]/xK)\}[[1-Lr]] \\ & + \{\cos^2(2\pi([K]+1)/xK)\}[[1-L(1-r)]] \end{aligned} \quad (192)$$

where

$$K = 2f_o/f_s \quad (193)$$

$$z = [K] \quad (194)$$

$$r = K - [K] \quad (195)$$

$$L = f_s/W \quad (196)$$

and $[]$ indicates the quantity is to be taken as zero if it is negative. Eq (192) holds for $L \leq 2f_0/W + 1$; for larger L , the error is zero.

This is the desired result. Note that substituting $x = 4$ into Eq (192) will yield the quadrature sampling error formula developed by Persons.

Given f_0 and W , Q can be plotted as a function of K for any L . As mentioned, Eq (192) provides us with the flexibility to investigate the effects of hardware timing errors on Q . If we use Persons' example we can establish it as a baseline (he assumed no timing error). In other words, we'll assume that we've sampled $f(t)$ and $f(t-1/4f_0)$ with no timing error. This is the case where $x = 4$. Letting $L = f_s/W = 1$ we have

$$Q(K, L+1) = \{\cos^2(\pi z/2K)\}[[1-r]] \\ + \{\cos^2(\pi(z+1)/2K)\}[[r]] \quad (197)$$

which is plotted in Figure 31. Figure 31a shows the full scale of Q for $0 \leq Q \leq 1.0$ where $1.0 = 100\%$ error. In part b the Q scale was expanded to emphasize the shape of the error plot. Notice that Q is zero for $K = \text{integer}$ and approaches zero for narrowband systems (large values of K).

$Q(K=2f_0/W, L=f_s/W=1)$ vs K

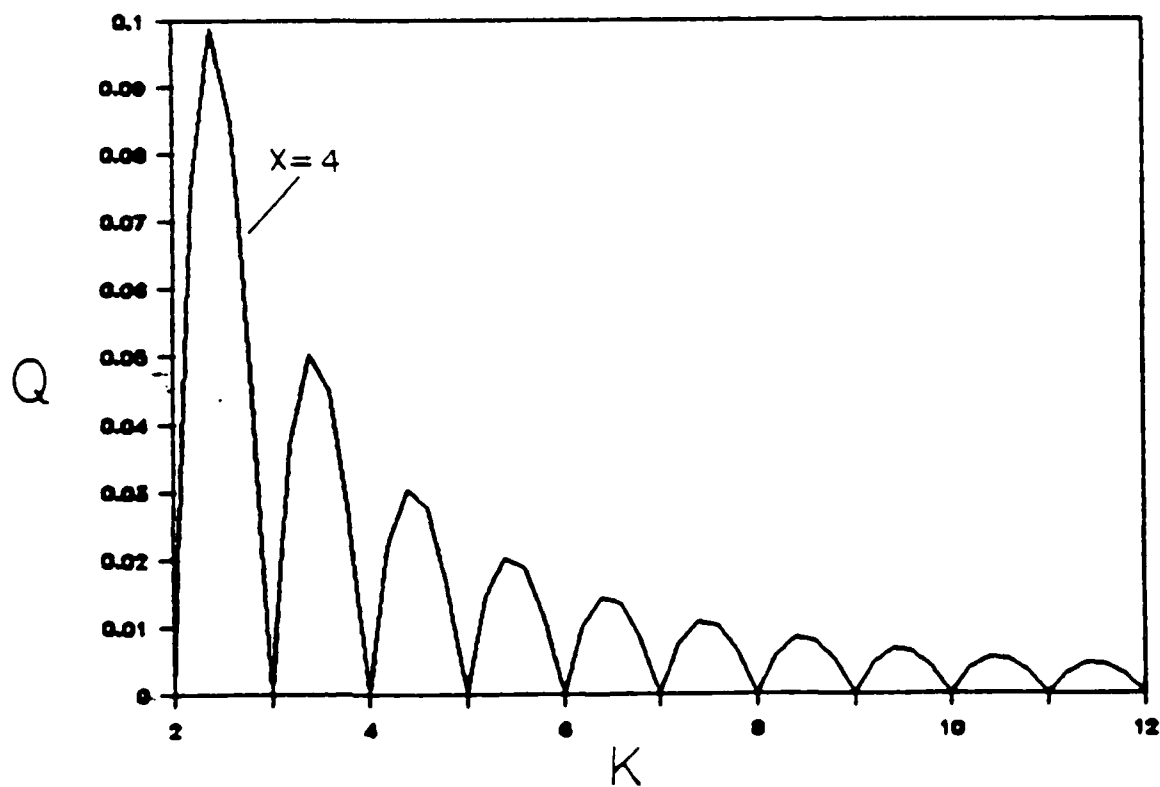
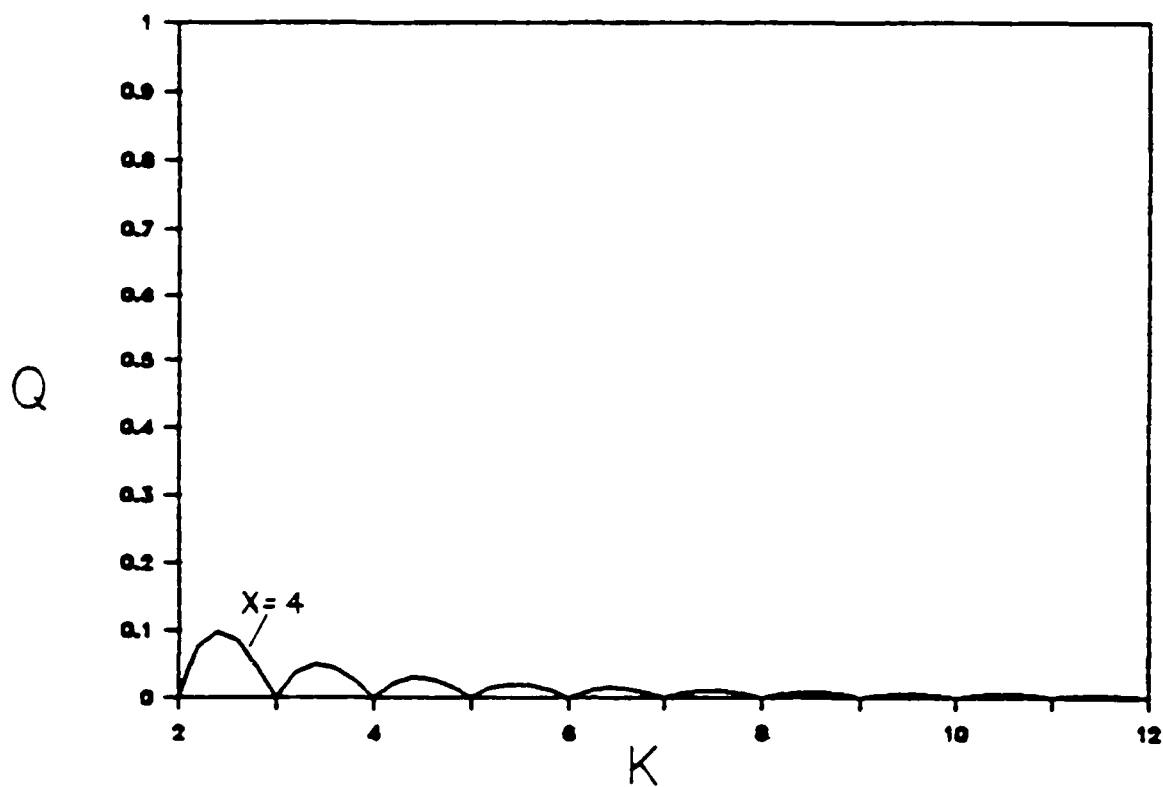


Figure 31. Q vs K with $L = 1.0$ - Persons' Example

The interesting question is, what happens to Q if we have a timing error? In other words, we think we're sampling $f(t)$ and $f(t-1/4f_0)$, but we're actually sampling $f(t)$ and $f(t-1/xf_0)$ where x does not equal 4. Since quadrature sampling requires sampling the bandpass signal and its quarter-wavelength translation, we expect some reconstruction error. The next few figures will show that there is indeed a reconstruction error and this error can be quite significant. For instance, if $x=2$ then the bandpass signal and its half-wavelength translation are being sampled and the reconstruction error approaches 100% (the signal cannot be reconstructed).

Q is plotted in Figure 32a for $x = 4.0, 3.9, 3.8, 3.7, 3.6, 3.5$ and $0 \leq Q \leq 1.0$ and once again in Figure 32b with $0 \leq Q \leq 0.16$. The individual plots for the various values of x are more easily distinguishable in part b. Notice as the timing error increases, or $|x-4.0|$ grows larger, that Q increases. Figure 33 shows the case where the timing error has increased to the point where we are sampling the bandpass waveform and its half-wavelength ($x = 2.0$). In this figure, Q is plotted with $x = 4.0, 3.8, 3.5, 3.0, 2.5, 2.0$. As before, Q approaches 100% as x approaches 2.0. Figure 33b is a three-dimensional surface plot of part a.

To summarize, consider an example with three high frequency bandpass signals with center frequencies of $f_1 = 40$ MHz, $f_2 = 500$ MHz, and $f_3 = 1$ GHz. Once again

$Q(K=2f_0/W, f_s=W=1)$ vs K

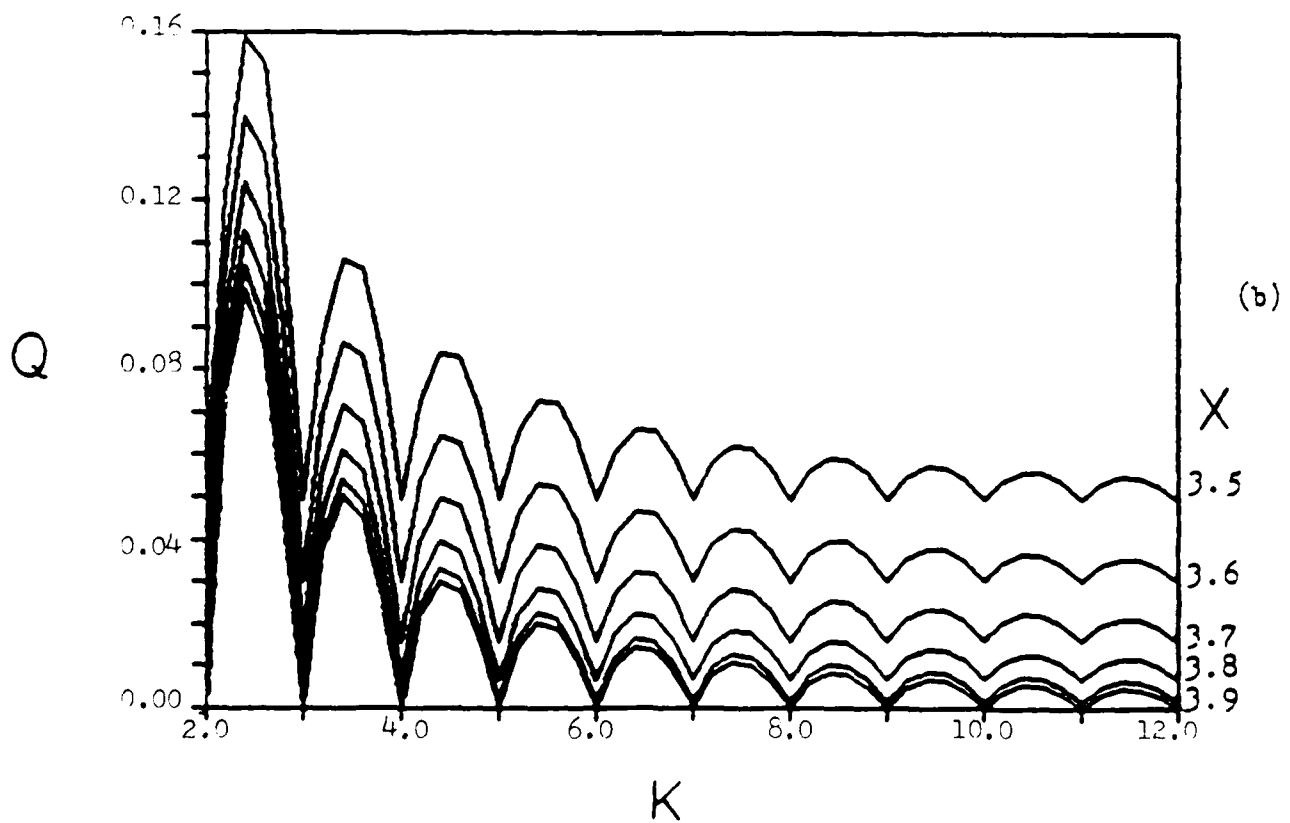
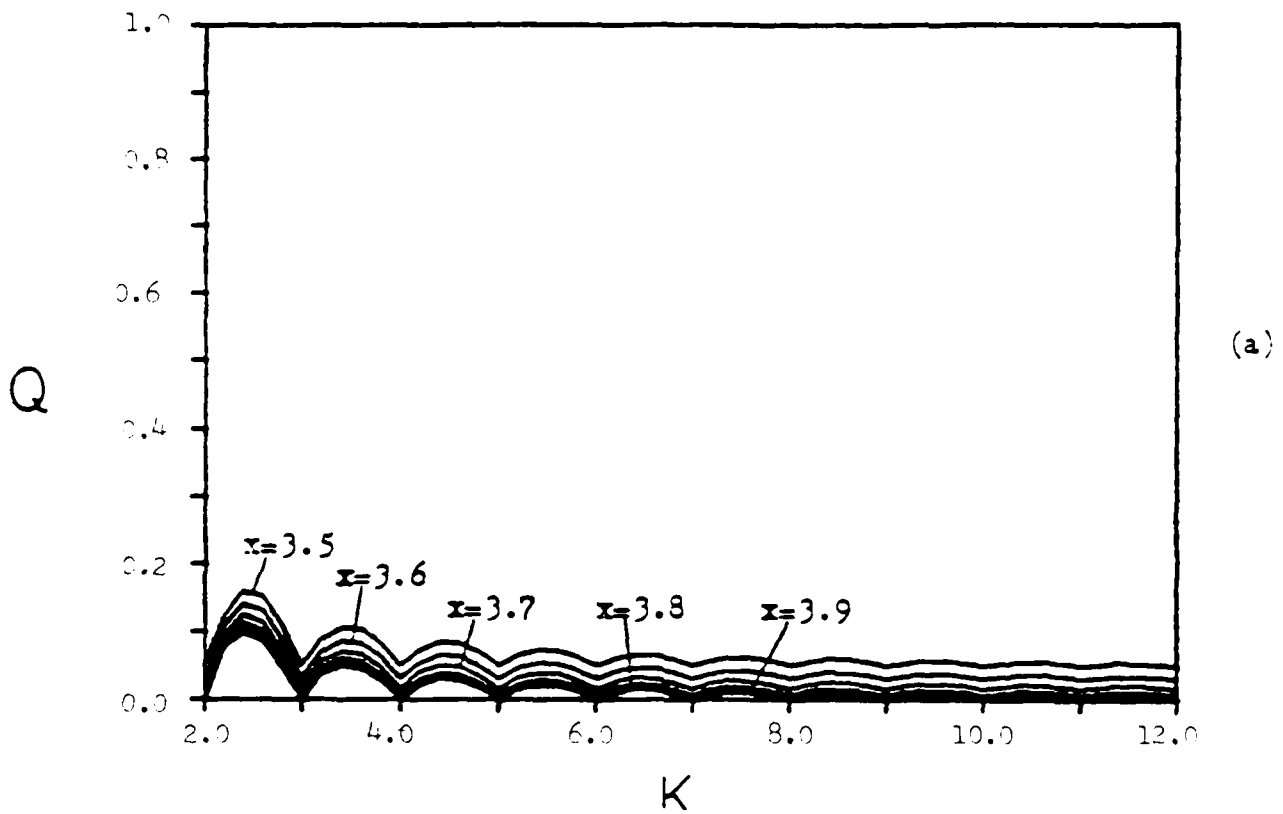


Figure 32. Q vs K with $L = 1.0$ - Small Timing Errors

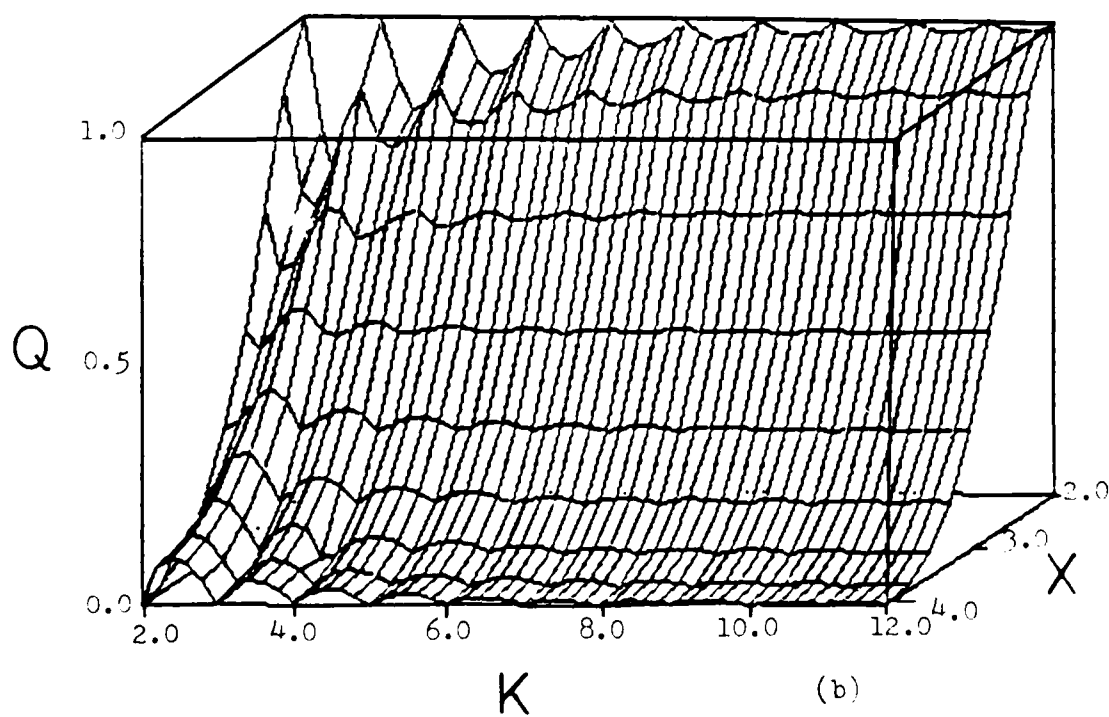
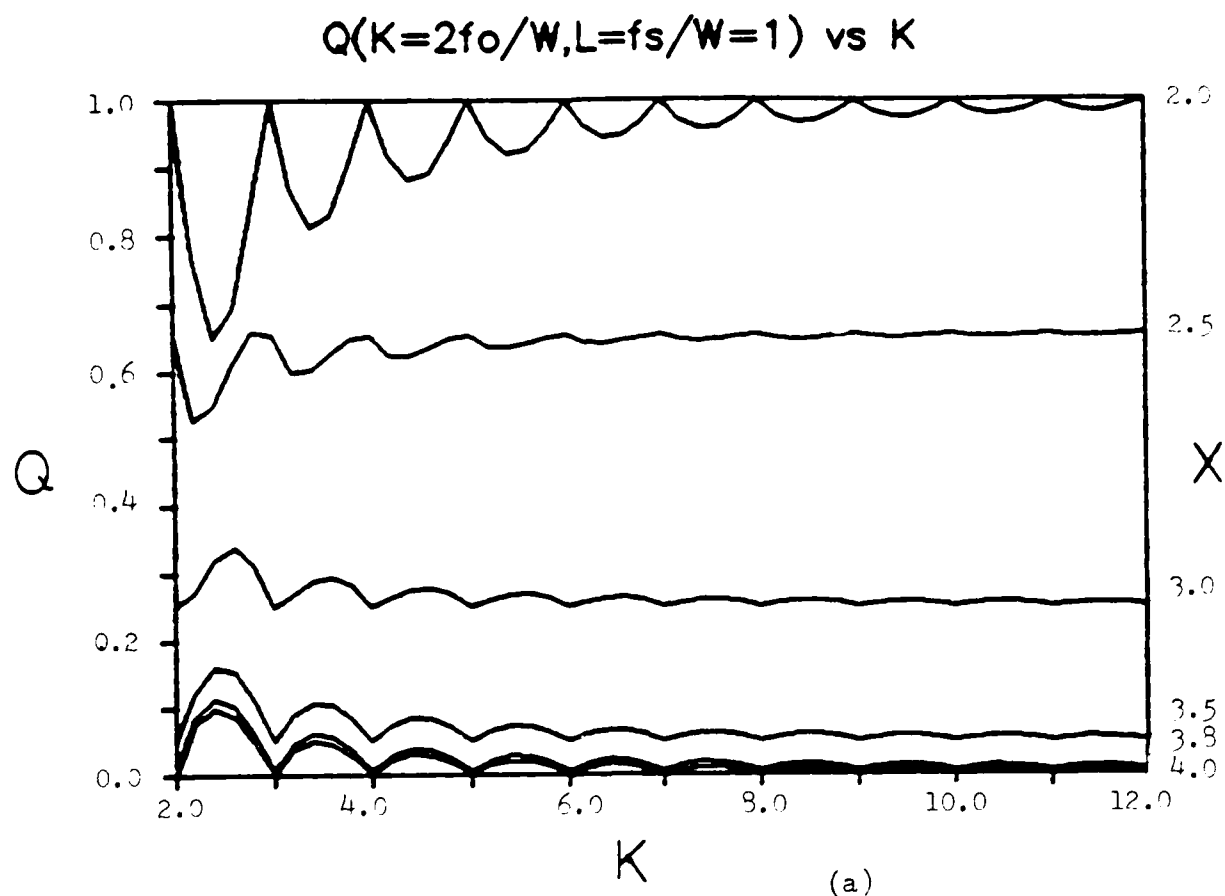


Figure 33. Q vs K with $L = 1.0$ - Large Timing Errors

TABLE I

Comparison of Timing Errors (T_E in pS)

X	T_E for		
	$f_1 = 40$ MHz	$f_2 = 500$ MHz	$f_3 = 1$ GHz
3.9	160	13	6
3.8	329	26	13
3.5	893	71	35
3.0	2083	167	83
2.5	3750	300	150
2.0	6250	500	250

$f_s = 1.5W$, $f_s = 2.0W$ and $f_s = 5.0W$ respectively. As the sampling rate grows large compared to the bandwidth the error terms approach zero. In Figure 36, Q is negligible for $x = 4.0$ (no timing error), 3.8 and 3.5 . The only significant Q terms are for $x = 3.0$, 2.5 and 2.0. Increasing sampling rates will reduce the Q terms even further.

To summarize, quadrature sampling requires very precise timing. Even with center frequencies less than 100 MHz, nanosecond precision is required. If such precision is not possible, higher sampling rates will be needed to overcome the reconstruction error terms.

let $L = 1 = f_s/W$. The timing errors, T_E , is a function of x :

$$T_E = T(1/4 - 1/x) \quad (198)$$

where T is the period of the corresponding bandpass signal.

In Figure 33, a value of $x = 2.0$ results in a Q of almost 1.0 (or 100%) . Referring to Table I, and putting this in terms of a timing error, we see that for f_1 , a T_E of only 6nS yields a Q of 100% . Similarly, $T_E = 500$ pS and 250 pS for f_2 and f_3 , respectively.

The important point here is that Q is directly proportional to the center frequency. The higher the center frequency, the more precise the timing must be to keep Q small.

Typical communication signals will be sampled at the IF stages of the receiver, so T_E for f_1 is representative of the type of timing precision needed for quadrature sampling when $f_s = W$ samples/s. Referring again to Figure 33 and looking at the column for f_1 in Table I, where $x = 3.8$, $T_E = 329$ pS and Q is relatively small for large values of K . A value of $x = 3.0$ represents a 2 nanosecond timing error and a Q that levels off at 0.3 (30%). Obviously, timing must be kept to nanosecond precision or it won't be possible to reconstruct the signal from the samples.

The next question is, what can be done to get around this timing problem? The answer is to sample at a higher rate. The next three figures (34-36) are plots of Q for

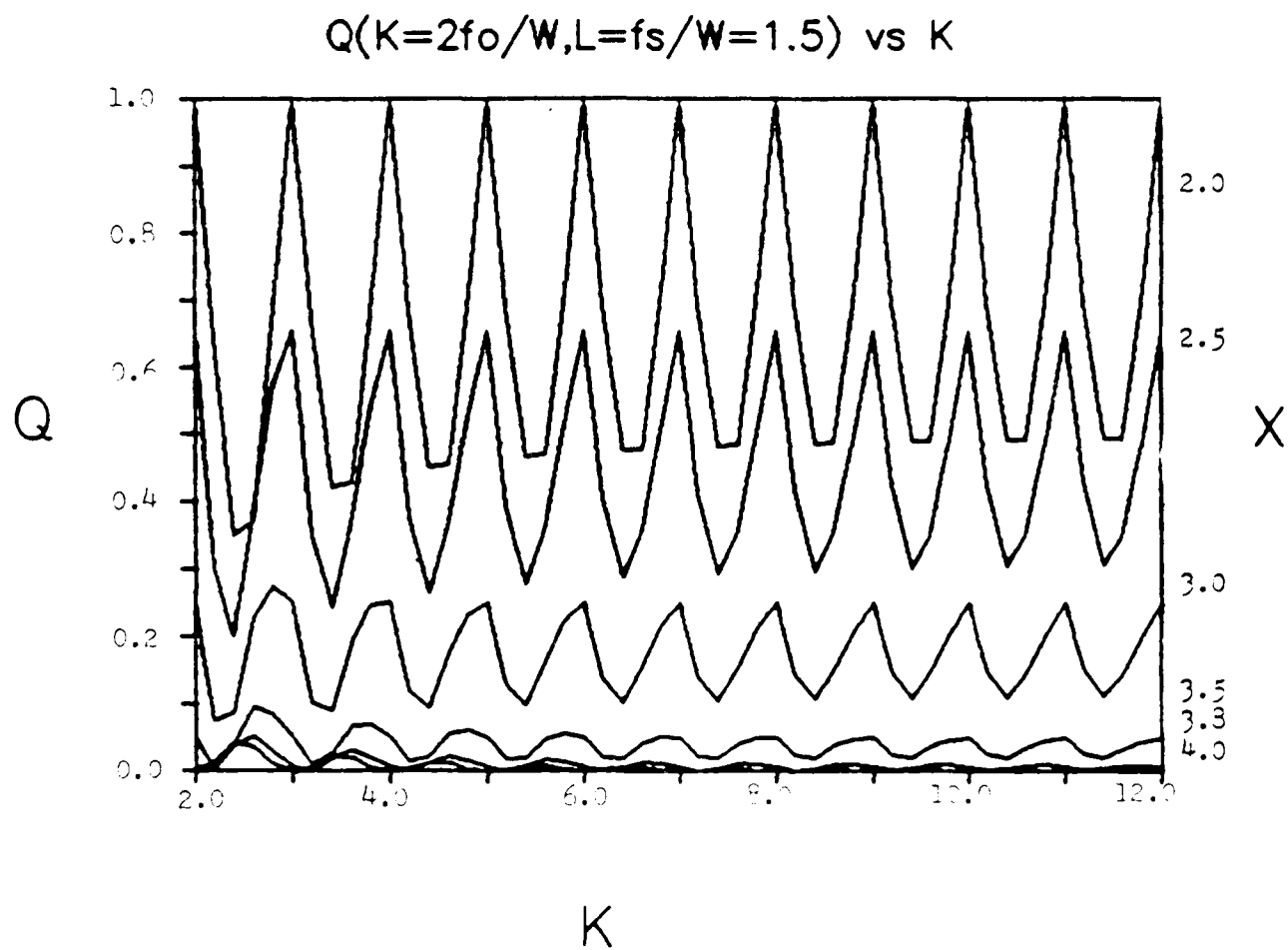


Figure 34. Q vs K with $L = 1.5$

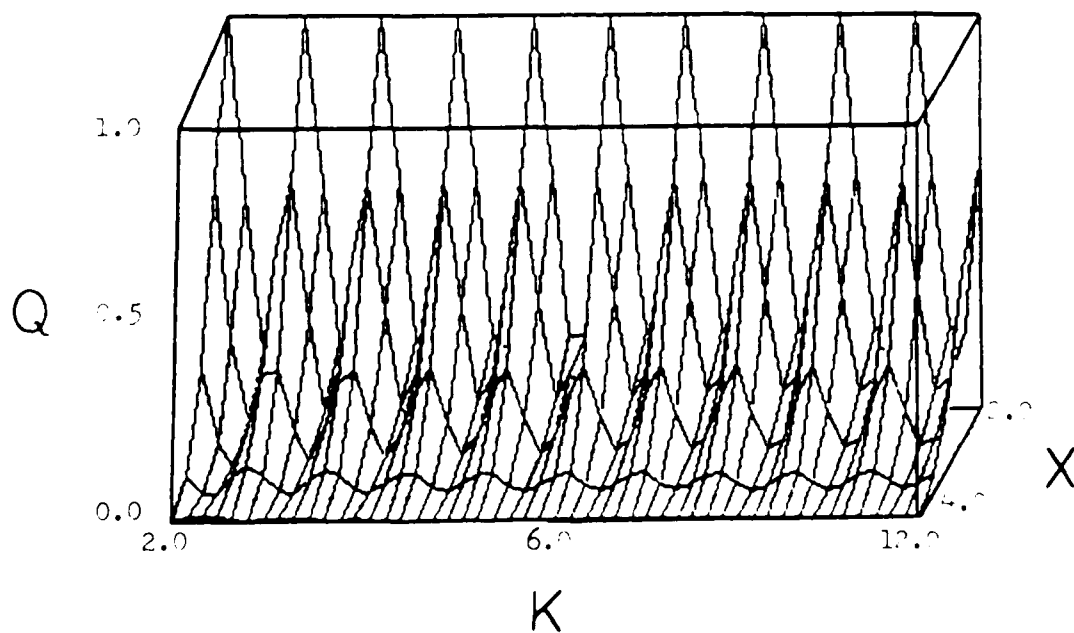
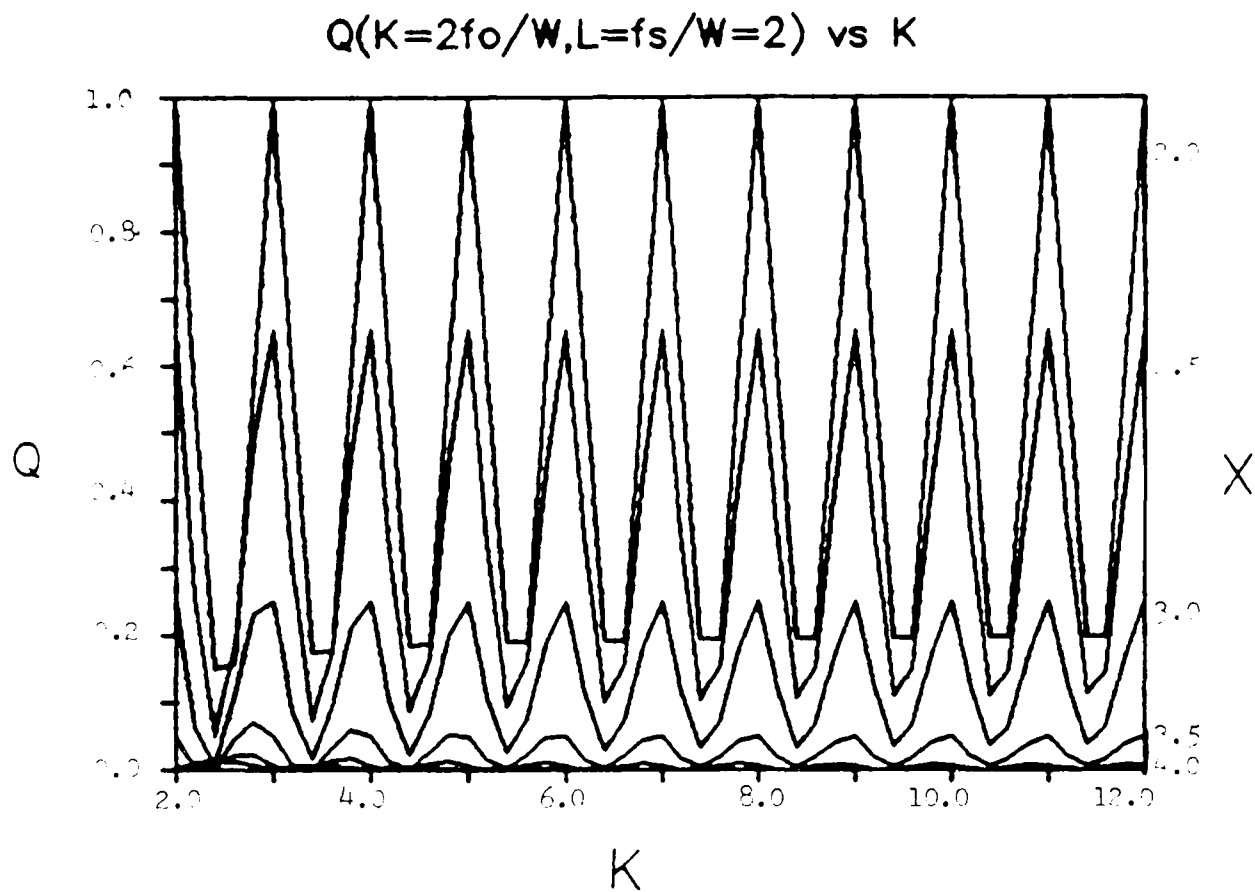


Figure 35. Q vs K with $L = 2.0$

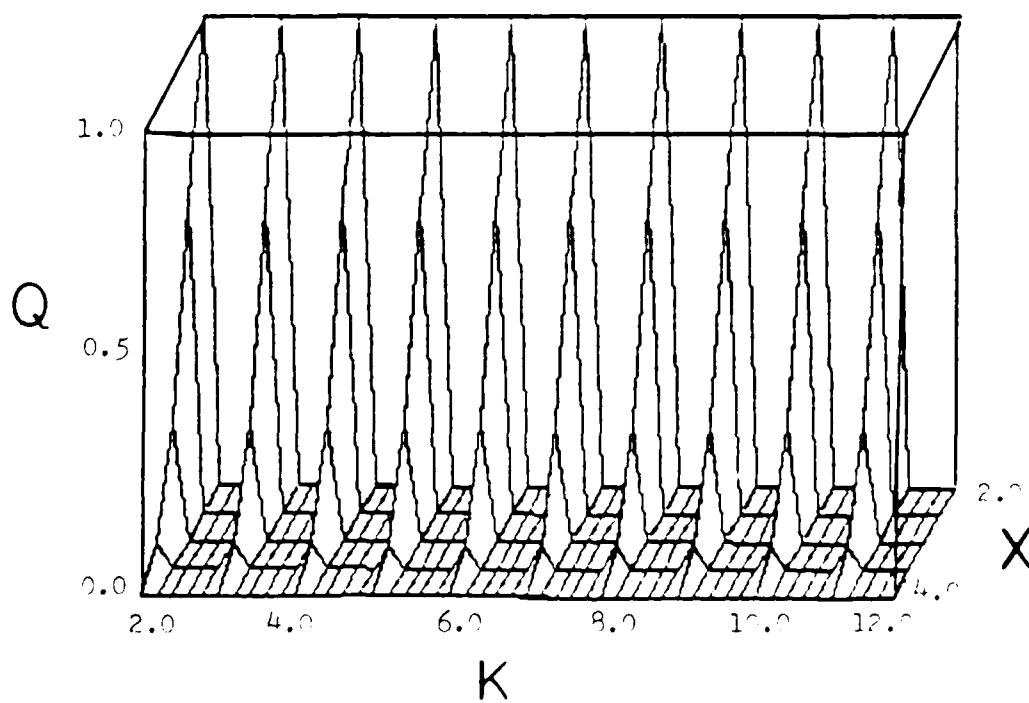
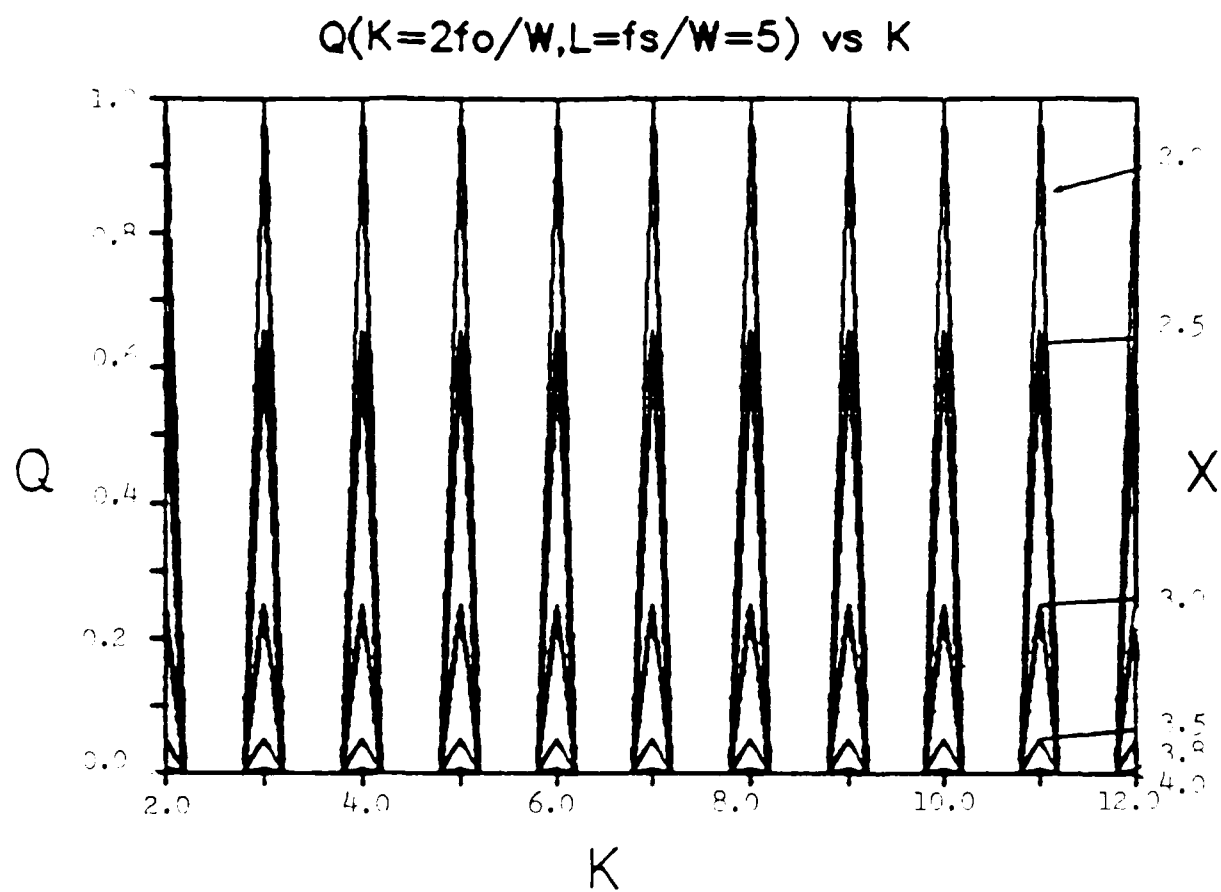


Figure 36. Q vs K with $L = 5.0$

Complex Sampling

The drawback of complex sampling is the preprocessing that must be done to obtain the Hilbert transform of the bandpass signal. There is the further disadvantage that it is not easy to obtain a precise Hilbert transform (the noncausality of the Hilbert transform does not allow one to implement it for signals having non-zero bandwidth, theoretically). Simpler processing is usually desirable (5:289).

IV. Conclusions and Recommendations

Conclusions

Five bandpass sampling techniques were evaluated. In each case, equations for the bandpass signal were developed in terms of its uniform samples. The minimum sampling rate and the conditions for those minimum sampling rates were discussed. In comparing sampling rates it was found that each of the two-channel techniques offered a rate reduction of up to one-half over the single-channel approach. There are always tradeoffs that result in varying degrees of accuracy and must be considered when determining which technique to use. For example, it was shown that conventional quadrature sampling requires precise synchronization, quadrature sampling was shown to be extremely sensitive to timing errors and is very hard to implement in hardware. It was concluded that the purpose for which the data will be used is the choice of sampling technique.

Recommendations

As the frequency of the signal to be sampled increases, the complexity of the sampling technique increases. It is recommended that the choice of sampling technique be based on the aspects of the signal to be sampled and the purpose for which the data will be used.

AD-A109 042

HIGH SPEED BANDPASS SAMPLING OF DIGITAL COMMUNICATIONS
WAVEFORMS(U) AIR FORCE INST OF TECH WRIGHT-PATTERSON
AFB OH SCHOOL OF ENGINEERING T E KEITH DEC 87

2/2

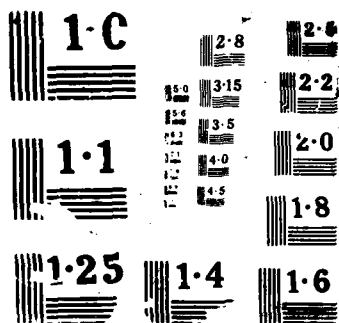
UNCLASSIFIED

AFIT/GE/ENG/870-31

F/G 14/2

NL





aspect which can be investigated is the reconstruction error due to the combined effects of hardware timing errors and varying levels of noise.

Bibliography

1. Brown, J.L. Jr. "On Quadrature sampling of Bandpass Signals," IEEE Transactions on Aerospace and Electronic Systems, AES-15: 366-371 (May 1979).
2. Brown, J.L. Jr. "A Simplified Approach to Optimum Quadrature Sampling," The Journal of the Acoustical Society of America, 67: 1659-1662 (December 1979).
3. Brown, J.L. Jr. "First-Order Sampling of Bandpass Signals - A New Approach," IEEE Transactions on Information Theory, 26: 613-615 (September 1980).
4. Cooper, George r. and Clare D. McGillem. Modern Communications and Spread Spectrum. New York: McGraw-Hill, Inc., 1986.
5. Figueiras-Vidal, Anibal R. "Sampling Bandpass Signals," IEEE Transactions on Aerospace and Electronic Systems, AES-17: 288-295 (March 1981).
6. Gagliardi, Robert Introduction To Communication Engineering. New York: John Wiley and Sons, 1978.
7. Grace, O.D. and Pitt, S.P. "Quadrature Sampling of High Frequency Waveforms," The Journal of the Acoustical Society of America, 44: 1453-1454 (March 1968).
8. Kohlenberg, Arthur. "Exact Interpolation of Band-Limited Functions," Journal of Applied Physics, 24: 1432-1436 (December 1953).
9. Oppenheim, Alan v. and Alan S. Willsky. Signals and Systems. Englewood Cliffs NJ: Prentice-Hall, Inc., 1983.
10. Peebles, Payton Z. Jr. Digital Communication Systems. Englewood Cliffs NJ: Prentice-Hall, Inc., 1987.
11. Persons, C.E. "Quadrature Sampling Error Formula," The Journal of the Acoustical Society of America, 57: 511-512 (November 1974).
12. Prescott, Glenn E. Class handout distributed in EENG 691, Digital Signal Processing, School of Engineering, Air Force Institute of Technology (AU), Wright-Patterson AFB OH, Fall quarter 1986.

13. Pridham, Roger G. and Mucci, Ronald A. "Digital Interpolation Beamforming for Low-Pass and Bandpass Signals," Proceedings of the IEEE, 67: 904-919 (June 1979).
14. Rife, Douglas D. "Aliasing: Causes and Cures," Personal Engineering and Instrumentation News, 51-54 (December 1986).
15. Roden, Martin S. Analog and Digital Communication Systems. Englewood Cliffs NJ: Prentice-Hall, Inc., 1979.
16. Stanley, William D. Digital Signal Processing. Reston VI: Reston Publishing Company, Inc, 1975.
17. Stremler, Ferrel G. Introduction to Communications Systems (Second Edition). Reading Massachusetts: Addison-Wesley Publishing Company, 1982.
18. Waters W.M. and B.R. Jarrett. "Bandpass Signal Sampling and Coherent Detection," IEEE Transactions on Aerospace and Electronic Systems, 4: 731-736 (November 1982).

VITA

Tommy E. Keith was born on 28 March 1955 in Midwest City, Oklahoma. He graduated from Ontario High School in Ontario, Ohio, in 1973 and enlisted in the United States Air Force in November 1974. He attended the University of Arkansas under the Airman Education and Commissioning Program and received the Bachelor of Science Degree in Electrical Engineering. Upon graduation in May 1983, he attended Officer Training School and received his commission in August 1983. From August 1983 to May 1984 he was assigned to the 554th Range Group at Nellis AFB, Nevada, where he worked as a project engineer. He served as a software evaluator for the Precision Location Strike System Test Team at Nellis AFB from May 1984 until entering the School of Engineering, Air Force Institute of Technology, in June 1986.

Permanent Address: 1381 N. Stewart Road
Mansfield, Ohio 44903

UNCLASSIFIED

SECURITY CLASSIFICATION OF THIS PAGE

REPORT DOCUMENTATION PAGE

Form Approved
OMB No. 0704-0188

1a. REPORT SECURITY CLASSIFICATION UNCLASSIFIED		1b. RESTRICTIVE MARKINGS	
2a. SECURITY CLASSIFICATION AUTHORITY		3. DISTRIBUTION / AVAILABILITY OF REPORT Approved for public release; distribution unlimited.	
2b. DECLASSIFICATION / DOWNGRADING SCHEDULE		5. MONITORING ORGANIZATION REPORT NUMBER(S)	
4. PERFORMING ORGANIZATION REPORT NUMBER(S) AFIT/GE/ENG/87D-31		5. MONITORING ORGANIZATION REPORT NUMBER(S)	
6a. NAME OF PERFORMING ORGANIZATION School of Engineering	6b. OFFICE SYMBOL (If applicable) AFIT/ENG	7a. NAME OF MONITORING ORGANIZATION	
6c. ADDRESS (City, State, and ZIP Code) Air Force Institute of Technology Wright-Patterson AFB, OH 45433-6583		7b. ADDRESS (City, State, and ZIP Code)	
8a. NAME OF FUNDING / SPONSORING ORGANIZATION Avionics Laboratory	8b. OFFICE SYMBOL (If applicable) AFWAL/AAAI-4	9. PROCUREMENT INSTRUMENT IDENTIFICATION NUMBER	
8c. ADDRESS (City, State, and ZIP Code) 1381 North Stewart Road Mansfield, OH 44903		10. SOURCE OF FUNDING NUMBERS	
		PROGRAM ELEMENT NO	PROJECT NO
		TASK NO	WORK UNIT ACCESSION NO
11. TITLE (Include Security Classification) see block 19			
12. PERSONAL AUTHOR(S) Amy E. Keith, B.S.E.E., Capt, USAF			
13a. TYPE OF REPORT MS Thesis	13b. TIME COVERED FROM _____ TO _____	14. DATE OF REPORT (Year, Month, Day) 1987 December	15. PAGE COUNT 101
16. SUPPLEMENTARY NOTATION			
17. COSATI CODES		18. SUBJECT TERMS (Continue on reverse if necessary and identify by block number)	
FIELD	GROUP	SUB-GROUP	
25	02		
		Bandpass Sampling, Direct Sampling, Quadrature Sampling, Second-order Sampling, Complex Sampling, Hilbert Sampling, pth-order Sampling	
19. ABSTRACT (Continue on reverse if necessary and identify by block number)			
Title: HIGH SPEED, BANDPASS SAMPLING OF DIGITAL COMMUNICATIONS WAVEFORMS			
Thesis Chairman: Glenn E. Prescott, Major, USAF Associate Professor of Electrical Engineering			
20. DISTRIBUTION / AVAILABILITY OF ABSTRACT <input checked="" type="checkbox"/> UNCLASSIFIED/UNLIMITED <input type="checkbox"/> SAME AS RPT <input type="checkbox"/> DTIC USERS		21. ABSTRACT SECURITY CLASSIFICATION UNCLASSIFIED	
22a. NAME OF RESPONSIBLE INDIVIDUAL Glenn E. Prescott, Major, USAF		22b. TELEPHONE (Include Area Code) 513-255-3576	22c. OFFICE SYMBOL AFIT/ENG

John W. ...
 Development
 Wright-Patterson AFB OH 45433

The purpose of this thesis is to investigate and analyze bandpass sampling techniques. Bandpass sampling theory is shown to be an extension of the Shannon low-pass sampling theory. Five bandpass sampling techniques are investigated: direct sampling (also called first-order sampling), p th-order sampling (in particular second-order sampling where $p=2$), conventional quadrature sampling, quadrature sampling, and complex sampling (also called Hilbert transform sampling).

Direct sampling is a single channel approach to bandpass sampling while the other approaches require two channels. The two channel techniques offer a sampling rate reduction of up to one half over direct sampling, but there are trade-offs to consider when choosing a two channel technique. It is shown that the effects of random phase error can render the conventional quadrature sampling approach useless. Timing is critical with quadrature sampling. Reconstruction error, due to hardware timing errors, is shown to be directly proportional to the center frequency and is a function of the bandwidth of the signal. Plots were developed to show the effect of timing on a given bandpass signal when the center frequency and the bandwidth are known.

END

DATE

FILMED

APRIL

1988

DTIC